

Entanglement spreading in a minimal model of maximal many-body quantum chaos

Bruno Bertini, Pavel Kos, and Tomaž Prosen¹

¹*Department of Physics, Faculty of Mathematics and Physics,
University of Ljubljana, Jadranska 19, SI-1000 Ljubljana, Slovenia*

The spreading of entanglement in out-of-equilibrium quantum systems is currently at the centre of intense interdisciplinary research efforts involving communities with interests ranging from holography to quantum information. Here we provide a constructive and mathematically rigorous method to compute the entanglement dynamics in a class of “maximally chaotic” periodically driven quantum spin chains. Specifically, we consider the so called “self-dual” kicked Ising chains initialised in a class of separable states and devise a method to compute exactly the time evolution of the entanglement entropies of finite blocks of spins in the thermodynamic limit. Remarkably, these exact results are obtained despite the models considered are maximally chaotic: their spectral correlations are described by the circular orthogonal ensemble of random matrices on all scales. Our results saturate the so called “minimal cut” bound and are in agreement with those found in the contexts of random unitary circuits with infinite-dimensional local Hilbert space and conformal field theory. In particular, they agree with the expectations from both the quasiparticle picture, which accounts for the entanglement spreading in integrable models, and the minimal membrane picture, recently proposed to describe the entanglement growth in generic systems.

CONTENTS

References

24

I. Introduction	1
II. Model, quench protocol, and observables of interest	2
III. Outline of the results	4
IV. Duality Mapping for the Entanglement Entropies	5
V. Separating states	10
VI. Entanglement spreading from separating states	10
A. Maximal eigenvalues of the transfer matrix	10
B. Entanglement dynamics	11
VII. Entanglement spreading from generic states	13
A. Generic case	14
B. Integrable case	15
VIII. Conclusions	15
Acknowledgements	16
A. Duality of traces	16
B. Simplified transfer matrix for longitudinal separating states	17
C. Proof of Property 1	18
D. Simplified commutation relations	19
E. Proof of Eqs. (82) and (83)	20
F. Proof of Property (80)	21
1. Proof of Lemma 1.	22

I. INTRODUCTION

Entanglement is arguably the most distinctive feature of quantum mechanics. It generates a special kind of non-local correlations which can be present in quantum states but have no analogues in the classical realm. While its elusive nature puzzled physicists for many years [1, 2], it is currently regarded as a powerful resource for advances both in technological applications and in the theoretical understanding of the physical world. In particular, it plays a crucial role in the study of quantum many-body systems out of equilibrium [3, 4]. This is due to two main reasons. First, the growth of entanglement during the non-equilibrium dynamics measures the increasing complexity of a time-evolving quantum state, with immediate implications on the feasibility of tensor network simulations [5–9]. Second, the evolution of the entanglement gives crucial information on how equilibrium statistical mechanics emerges from many-body quantum dynamics. Specifically, it is now understood that the thermodynamic entropy of the statistical ensemble describing local observables at infinite times is a measure of the entanglement accumulated during the time evolution [10–14].

Moreover, the very way in which the entanglement spreads for finite times appears to be among the most universal aspects of many-body dynamics. Consider for instance an initial separable state, where none of the local constituents is entangled with any other. Switching on spatially local Hamiltonian interactions throughout the system (a procedure called “global quench”), one finds quite generally that the bipartite entanglement between a large connected region of the system and the rest grows linearly in time. This scenario has been observed in a large number of analytical and numerical in-

vestigations [15–43] and recently even in cold atomic experiments [44]. Known exceptions to this empirical fact are systems exhibiting real space localization [16, 45], confinement [46], and quenched disorder creating weak links [47]. In particular, the logarithmic spreading of entanglement in the presence of many-body localization (MBL) [48] is one of the main defining features of the MBL phase.

The linear growth of entanglement after a global quench has been first observed in the context of $(1+1)$ -dimensional conformal field theory (CFT), where it has been explained in terms of an intuitive quasiparticle picture [15]. The initial state, which is not an eigenstate of the Hamiltonian, can be thought of as a collection of pairs of oppositely moving quasiparticles. These, in the course of time, spread the entanglement across the system, in a similar way to the one conceived in the historical gedanken experiment by Einstein, Podolsky and Rosen [1]. In this picture, the entanglement between two different portions of the system is given by the number of pairs sharing a particle with each portion. The same idea can be used to explain the entanglement spreading in systems with stable quasiparticle excitations, for instance free [17] and interacting [26] integrable models. It does not account, however, for the linear growth of entanglement observed in systems with no identifiable quasiparticle content such as generic interacting systems [41–43] or holographic CFTs [33–36].

More recently, a fruitful avenue of research came from the study of the so-called random quantum circuits [47, 49–54], where the dynamics is completely random in space and the only constraint is given by the locality of interactions. In this case the linear growth of entanglement can be explained using a “minimal membrane” picture [49, 52], which is conjectured to apply, at least at the qualitative level, to generic (non-integrable) clean and noisy systems in any spatial dimension. In essence one quantifies the amount of entanglement between two portions of the system by measuring the surface of the minimal space-time membrane separating the two portions. This picture has been analytically tested in certain limiting regimes of the random quantum circuits, specifically assuming that the Hilbert space dimension q per local constituent is large ($q \gg 1$). Results are available both when the dynamics are random also in time [49, 53], and when they are periodically driven [54]. No analytical result, however, exists on entanglement dynamics in specific non-integrable models with local interactions and small finite q or, in general, for clean systems.

In this paper we fill this gap providing exact results for the entanglement dynamics for a quantum chaotic spin chain with two-dimensional local Hilbert space ($q = 2$). Specifically, we consider a family of Floquet-Ising chains which undergo a transition between integrability and ergodicity (or quantum chaos) by turning on a longitudinal magnetic field. The latter may be either spatially homogeneous or arbitrarily spatially modulated. Note that the non-integrability of the model for non vanish-

ing longitudinal magnetic fields has recently been proved by computing exactly the spectral statistics [55]. We identify a class of separable initial states, homogeneous or arbitrarily modulated in space, from which the entanglement dynamics can be computed exactly for any non-disjoint bipartition. These results are of high significance for three main reasons. (i) They provide an exact verification of both the linear growth of entanglement and its relaxation to the thermodynamic entropy in a concrete quantum chaotic model. (ii) They provide a general method allowing to obtain exact results for the non-equilibrium dynamics of many-body quantum systems even in the absence of integrability. (iii) They are valid in both the integrable and the non-integrable case, allowing for a unified interpretation of the entanglement spreading.

The paper is laid out as follows. In Sec. II we introduce the model considered, define the protocol used to drive it out of equilibrium, and introduce the entanglement measures of interest. In Sec. III we present a comprehensive summary our results. In Sec. IV we explain the duality mapping which is the key for our analytical calculations. In Sec. V we identify the classes of initial states leading to an exactly solvable entanglement dynamics. In Sec. VI we sketch the main steps of the calculation. In Sec. VII we present numerical results for generic separable initial states. Finally, Sec. VIII contains our conclusions. A number of technical points and proofs are reported in the appendices.

II. MODEL, QUENCH PROTOCOL, AND OBSERVABLES OF INTEREST

The main objective of this paper is to determine a minimal quantum chaotic model [56], with local interactions and finite local Hilbert space, allowing for an exact determination of the entanglement spreading. A candidate emerging naturally in our quest is the so called kicked Ising model [57–59], which describes a classical Ising model in the presence of a longitudinal magnetic field and periodically kicked with a transverse magnetic field. This model is quantum chaotic in the sense that its spectral statistics are described by the circular orthogonal ensemble of random matrices [60], but, as we recently proved [55], at some specific points of its parameter space it allows for exact calculations. This is because at these points, called “self-dual” points (see below), the system acquires a remarkable algebraic structure making of it a *maximal scrambler with local interactions*.

To be more specific, let us introduce the Hamiltonian of the kicked Ising model. Setting to one the time interval between the kicks we have

$$H_{\text{KI}}[\mathbf{h}; t] = H_{\text{I}}[\mathbf{h}] + \sum_{m=-\infty}^{\infty} \delta(t - m) H_{\text{K}}, \quad (1)$$

where $\delta(t)$ is the Dirac delta function and we defined

$$H_I[\mathbf{h}] \equiv J \sum_{j=1}^L \sigma_j^z \sigma_{j+1}^z + \sum_{j=1}^L h_j \sigma_j^z, \quad (2)$$

$$H_K \equiv b \sum_{j=1}^L \sigma_j^x. \quad (3)$$

In these equations L is the volume of the system, the matrices σ_j^a , with $a \in \{x, y, z\}$, are the Pauli matrices at position j , and we use periodic boundary conditions adopting the notation convention $\sigma_{L+1}^a \equiv \sigma_1^a$.

The parameters J and b are, respectively, the Ising coupling and the transverse ‘‘kicking’’ field, while the L -component vector $\mathbf{h} = (h_1, \dots, h_L)$ describes a position dependent longitudinal field. As anticipated before, in this paper we consider some specific points in the parameter space of the model. In particular we focus on the ‘‘self-dual’’ points, specified by the condition

$$|J| = |b| = \frac{\pi}{4}. \quad (4)$$

As explained in Secs. IV, V, and VI, at these points a duality symmetry of the model allows for an analytical treatment of the entanglement dynamics. To be specific, from now on we set

$$J = \frac{\pi}{4}, \quad b = -\frac{\pi}{4}, \quad (5)$$

but our results apply to all the four combinations fulfilling (4). The longitudinal magnetic fields \mathbf{h} are instead left arbitrary and are used to switch between the integrable and the non-integrable case. Indeed, for $\mathbf{h} = \mathbf{0}$ the Hamiltonian (1) is integrable, while it is non integrable for a generic choice of longitudinal fields. In the latter case the only symmetry of (1) is the time reversal T , defined by its action on the spin variables as follows

$$\sigma_j^a \mapsto T \sigma_j^a T = \sigma_j^{a*}. \quad (6)$$

Here $(\cdot)^*$ denotes the complex conjugation in the ‘‘computational’’ basis, composed by simultaneous eigenstates of $\{\sigma_j^z\}$ for all j in $\{1, 2, \dots, L\}$

$$\mathcal{B}_L = \{|\mathbf{s}\rangle = |s_1, \dots, s_L\rangle, s_j \in \{\pm 1\} : \sigma_j^z |\mathbf{s}\rangle = s_j |\mathbf{s}\rangle\}. \quad (7)$$

In this paper we interchangeably use $s = +1 \equiv \uparrow$ and $s = -1 \equiv \downarrow$ to designate eigenvalues of Pauli matrices.

The Floquet operator generated by (1) reads as

$$U_{\text{KI}}[\mathbf{h}] = \mathfrak{T} \exp \left[-i \int_0^1 dt H_{\text{KI}}[\mathbf{h}; t] \right] = e^{-iH_K} e^{-iH_I[\mathbf{h}]}, \quad (8)$$

where $\mathfrak{T} \exp[\cdot]$ denotes a time-ordered exponential.

To drive the system out of equilibrium we consider a global quantum quench protocol: we initialise the system in the ground state of a short-range Hamiltonian and suddenly, say at $t = 0$, we start evolving with (1).

In particular, here we consider the ground states $|\psi_{\boldsymbol{\theta}, \boldsymbol{\phi}}\rangle$ of the following family of local, non-interacting, magnetization Hamiltonians

$$H_{\boldsymbol{\theta}, \boldsymbol{\phi}} = - \sum_{j=1}^L g_j \vec{n}_{\boldsymbol{\theta}_j, \boldsymbol{\phi}_j} \cdot \vec{\sigma}_j, \quad (9)$$

where $\boldsymbol{\theta} = (\theta_1, \dots, \theta_L)$ and $\boldsymbol{\phi} = (\phi_1, \dots, \phi_L)$ are L -component vectors with components $\theta_j \in [0, \pi]$ and $\phi_j \in [0, 2\pi]$, while $g_j > 0$ is arbitrary, and

$$\vec{n}_{\boldsymbol{\theta}, \boldsymbol{\phi}} = (\sin \theta \cos \phi, \sin \theta \sin \phi, \cos \theta), \quad (10)$$

is the radial unit vector in the three-dimensional space.

The ground states $|\psi_{\boldsymbol{\theta}, \boldsymbol{\phi}}\rangle$ of (9) are separable (*i.e.* they have zero entanglement): the spin at site j points in the direction $\vec{n}_{\boldsymbol{\theta}_j, \boldsymbol{\phi}_j}$ of its Bloch’s sphere. Namely, the states $|\psi_{\boldsymbol{\theta}, \boldsymbol{\phi}}\rangle$ are explicitly written as

$$|\psi_{\boldsymbol{\theta}, \boldsymbol{\phi}}\rangle = \bigotimes_{j=1}^L \left[\cos\left(\frac{\theta_j}{2}\right) |\uparrow\rangle + \sin\left(\frac{\theta_j}{2}\right) e^{i\phi_j} |\downarrow\rangle \right]. \quad (11)$$

After t periods of the Floquet evolution the state of the system then reads

$$|\psi_{\boldsymbol{\theta}, \boldsymbol{\phi}}(t)\rangle = (U_{\text{KI}}[\mathbf{h}])^t |\psi_{\boldsymbol{\theta}, \boldsymbol{\phi}}\rangle. \quad (12)$$

We stress that this protocol is constructive and simple enough to be realizable experimentally, for instance in the context of cold atoms [61–63].

In this work, the dynamics of the system are characterised by studying the time evolution of the entanglement between a contiguous subset of N spins $A = \{1, 2, \dots, N\}$ and the rest of the system, see Fig. 1. This is encoded in the density matrix of the system reduced to the subsystem A , defined as

$$\rho_A(t) = \text{tr}_{\mathcal{H}_{L-N}} [|\psi_{\boldsymbol{\theta}, \boldsymbol{\phi}}(t)\rangle \langle \psi_{\boldsymbol{\theta}, \boldsymbol{\phi}}(t)|], \quad (13)$$

where \mathcal{H}_{L-N} is the Hilbert space associated with the complement $A^c = \{N+1, \dots, L\}$ of A . The entanglement content of $\rho_A(t)$ is quantified by the Rényi entropies $S_A^{(n)}(t)$, also called entanglement entropies. These are a one-parameter family of functionals of $\rho_A(t)$ defined as follows

$$S_A^{(n)}(t) = \frac{1}{1-n} \log \text{tr} [(\rho_A(t))^n], \quad n \in \mathbb{N}. \quad (14)$$

In summary: in this paper we study the time evolution generated by (1) of the Rényi entropies (14) for a



FIG. 1. The partition of the spin chain considered in the calculation of the entanglement.

system initialised in the states $|\psi_{\theta,\phi}\rangle$. As we shall see, our analytical results apply in the thermodynamic limit $L \rightarrow \infty$. We stress that, in contrast with what we did elsewhere [55], we do not introduce any averaging on the longitudinal magnetic fields. The thermodynamic limit is taken for fixed initial state and time-evolving Hamiltonian.

III. OUTLINE OF THE RESULTS

Our main result consists in finding two specific but physically interesting subclasses of the states (11) for which the time evolution of all Rényi entropies in the thermodynamic limit can be found exactly, for any configuration of magnetic fields $\{h_j\}$ and subsystem size N . These special classes of states are defined as

$$\mathcal{T} = \{|\psi_{\frac{\pi}{2}\mathbf{1},\phi}\rangle, \quad \phi_j \in [0, 2\pi]\}, \quad (15)$$

$$\mathcal{L} = \{|\psi_{\bar{\theta},\phi}\rangle, \quad \bar{\theta}_j \in \{0, \pi\}\}, \quad (16)$$

where $\mathbf{1}$ denotes a vector of length L with all entries equal to 1 [65]. We respectively name them “transverse separating states” and “longitudinal separating states”, while we generically call “separating state” a state belonging to either \mathcal{T} or \mathcal{L} . These states are called “transverse” and “longitudinal” because they are respectively eigenstates of the operators $\cos \phi_j \sigma_j^x + \sin \phi_j \sigma_j^y$ and σ_j^z for all j s. Therefore, they can be thought of as configurations of a magnet where the spins lie on the x - y plane (“transverse plane”) or along the z axis (“longitudinal axis”). The adjective “separating” refers to their key mathematical property and it is thoroughly explained in Sec. V. Specific instances of states in \mathcal{T} and \mathcal{L} , which are most relevant from the experimental point of view, are the ground states of the two parts in the Floquet protocol. For example, when $J > 0$ and $|h_j| < J$ the ground state of H_I is $|\psi_{\pi\mathbf{1},\mathbf{0}}\rangle \in \mathcal{L}$, while when $b > 0$, the ground state of H_K is $|\psi_{\frac{\pi}{2}\mathbf{1},\pi\mathbf{1}}\rangle \in \mathcal{T}$.

To simplify the analysis of the results it is useful to note that the time evolution of the states in \mathcal{L} can be related to that of those in \mathcal{T} . This is easily seen by means of the following identity

$$|\psi_{\bar{\theta},\phi}(1)\rangle = U_{\text{KI}}[\mathbf{h}]|\psi_{\bar{\theta},\phi}\rangle \simeq |\psi_{\psi_{\frac{\pi}{2}\mathbf{1},\bar{\theta}-\frac{\pi}{2}\mathbf{1}}}\rangle, \quad (17)$$

where \simeq denotes equality up to a global phase. This identity is proven by observing that, since the states in \mathcal{L} are eigenstates of σ_j^z , they are also eigenstates of $H_I[\mathbf{h}]$. Therefore the application of $e^{-iH_I[\mathbf{h}]}$ only changes $|\psi_{\bar{\theta},\phi}\rangle$ by a global phase. Moreover, an explicit calculation shows that

$$e^{-iH_K}|\psi_{\bar{\theta},\phi}\rangle \simeq |\psi_{\psi_{\frac{\pi}{2}\mathbf{1},\bar{\theta}-\frac{\pi}{2}\mathbf{1}}}\rangle. \quad (18)$$

Eq. (17) means that the first time step of evolution for states in \mathcal{L} keeps them in a separable form, and hence

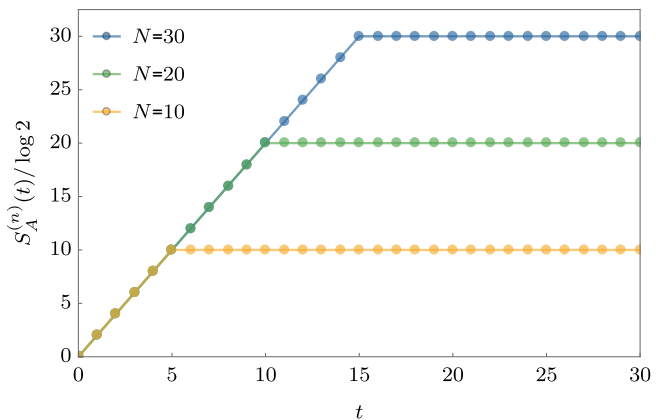


FIG. 2. Plot of the exact result of all Rényi entropies given by (21) for $\theta = \pi/2$ case. The expressions for $\theta = 0$ are delayed by one period.

does not change the entanglement, but turns them into states in \mathcal{T} . An immediate consequence of Eq. (17) is

$$|\psi_{\bar{\theta},\phi}(t)\rangle \simeq |\psi_{\frac{\pi}{2}\mathbf{1},\bar{\theta}-\frac{\pi}{2}\mathbf{1}}(t-1)\rangle, \quad t \geq 1. \quad (19)$$

Considering the entanglement entropy we then have

$$S_A^{(n)}(t)|_{\bar{\theta},\phi} = S_A^{(n)}(\max(t-1, 0))|_{\frac{\pi}{2}\mathbf{1},\bar{\theta}-\frac{\pi}{2}\mathbf{1}}, \quad t \geq 0, \quad (20)$$

where we explicitly reported the initial state dependence and used $S_A^{(n)}(0) = 0$. By virtue of this simple argument we can restrict our attention to the states in \mathcal{T} , the time evolution of the entropy for the states in \mathcal{L} is found using Eq. (20).

The time evolution of entanglement entropies from states in \mathcal{T} (in the thermodynamic limit) can be explicitly determined by means of the “duality method” developed in Secs. IV–VI. The result reads as

$$\lim_{L \rightarrow \infty} S_A^{(n)}(t) = \min(2t, N) \log 2. \quad (21)$$

This result is indisputably remarkable: when evolving from separating states all entanglement entropies take the same universal form, independent of the fields h_j and of details of the initial states. In particular, at fixed N , the entanglement entropies display a linear growth in time up to a non-analytic saturation point where they become constant, see Fig. 2. The independence of n of the result means that the spectra of the reduced density matrices $\rho_A(t)$ are *flat*. In other words the reduced density matrices have exactly $e^{S_A(t)}$ eigenvalues equal to $e^{-S_A(t)}$ while the other eigenvalues vanish.

Note that the form (21) for the evolution of the entanglement entropies has been found in a number of different physical settings, both in closed and periodically driven systems. Examples range from conformal invariant systems [15, 33], to non-integrable closed systems [42]. From random in time [49–51], to periodically driven [54] random unitary circuits. In particular, it saturates the

bound given by the “minimal cut” argument [34], namely

$$S_A^{(n)}(t) \leq \ell_{\min} \log q, \quad \forall n, \quad (22)$$

where q is the dimension of the local Hilbert space (2 in our case) and ℓ_{\min} is the minimal number of links intersected by a cut separating the region A from the rest of the system in a tensor network representation of the state at time t . This means that the exact result (21) agrees with the “minimal membrane” picture recently put forward in Ref. [49], where a form like (21) has been proposed to describe the leading-order features of single-interval entanglement dynamics in generic systems. Interestingly, however, our system also contains an integrable point, namely $\mathbf{h} = 0$. At this point our result agrees with the quasiparticle picture of Ref. [15], because in our case all quasiparticles move at the same, maximal, speed ($|v| = 1$).

We stress that, as opposed to all the other instances of a form like (21) mentioned above, our result does not hold only at the leading order for large t and N . It holds with no corrections for any t and N . This gives further evidence for the special status of the self-dual kicked Ising model as minimal solvable model for quantum chaos.

If the initial state is not separating the problem does not appear to be amenable to an analytical treatment and it is studied numerically, for a finite volume L , in Sec. VII. For $t \ll L$, the qualitative behaviour of the entropies remains similar in the integrable and non-integrable cases: we again observe a linear growth followed by saturation. There are, however, two remarkable differences. First, the saturation values in the two cases differ. While in the integrable case they retain memory of the initial states, in the non-integrable case the entropies always saturate to the universal value $N \log 2$, in agreement with quantum ergodicity. The slope of the short time growth, however, is generically smaller than $2 \log 2$, i.e. the maximal one. Rescaling the entropies by N and extrapolating the finite N data to $1/N \rightarrow 0$ we cannot, however, exclude a collapse to the maximal slope in the scaling limit $N, t \rightarrow \infty$. The second difference is that in the integrable case we observe recurrences due to finite sizes when $t \sim L$, in accord with the quasiparticle picture. In the non-integrable case these recurrences are, instead, absent (or at least negligible), in accord with the membrane picture.

IV. DUALITY MAPPING FOR THE ENTANGLEMENT ENTROPIES

In Ref. [64] the authors pointed out that the traces of integer powers of the Floquet operator (8) enjoy a useful space-time “duality symmetry”. This symmetry can be demonstrated as follows. First note that

$$\text{tr} [(U_{\text{KI}}[\mathbf{h}])^t], \quad t \in \mathbb{N}, \quad (23)$$

can be represented as a partition function of a classical Ising model on a $t \times L$ lattice, where $U_{\text{KI}}[\mathbf{h}]$ acts as transfer matrix in time, see Fig. 3 for a pictorial representation

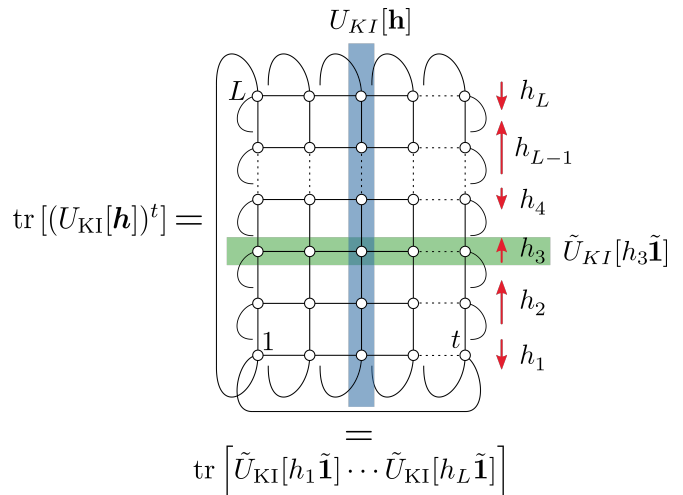


FIG. 3. Pictorial representation of the duality relation (24) fulfilled by the Floquet operator (8). Traces of powers of the Floquet operator correspond to the partition function of a classical Ising model on a $t \times L$ lattice. The column-to-column transfer matrix is given by $U_{\text{KI}}[\mathbf{h}]$ while the row-to-row transfer matrix between the $(j-1)$ -th and the j -th row is given by $\tilde{U}_{\text{KI}}[h_j \tilde{\mathbf{1}}]$. Note that self-duality condition implies that both transfer matrices are unitary.

and Appendix A for the explicit expression. Second, observe that, due to the short-range nature of the couplings in (2) and (3), the same quantity can also be written in terms of a transfer matrix defined on a lattice of t sites and propagating in space (see Appendix A). Namely we have

$$\text{tr} [(U_{\text{KI}}[\mathbf{h}])^t] = \text{tr} [\tilde{U}_{\text{KI}}[h_1 \tilde{\mathbf{1}}] \cdots \tilde{U}_{\text{KI}}[h_L \tilde{\mathbf{1}}]], \quad (24)$$

where “tilded” bold symbols denote vectors of t components, in particular $\tilde{\mathbf{1}} = (1, \dots, 1)$ has all entries equal to 1, and $\tilde{U}_{\text{KI}}[\tilde{\mathbf{h}}]$ is the transfer matrix in space, also known as dual transfer matrix. It turns out that $\tilde{U}_{\text{KI}}[\tilde{\mathbf{h}}]$ has the same form as the Floquet operator (8) (with L replaced by t in (2) and (3)) where the longitudinal magnetic field vector is given by $\tilde{\mathbf{h}}$, while Ising coupling \tilde{J} and the transverse field \tilde{b} are given by the following functions of J and b

$$\tilde{J} = -\frac{\pi}{4} - \frac{i}{2} \log \tan b, \quad (25)$$

$$\tilde{b} = -\frac{\pi}{4} - \frac{i}{2} \log \tan J. \quad (26)$$

Since \tilde{J} and \tilde{b} are generically complex, the transfer matrix $\tilde{U}_{\text{KI}}[\tilde{\mathbf{h}}]$ is generically not unitary. The dual couplings become real only when the model is at one of the self-dual points (4).

In Ref. [55] we showed that such duality symmetry can be used to compute non-trivial observables, considering the example of the disorder averaged spectral form factor. In that case, even if the quantity cannot be written in

terms of a transfer matrix in time, it can still be written in terms of a transfer matrix in space. This allowed us to perform an analytical calculation. The unitarity of the matrix $\tilde{U}_{\text{KI}}[\mathbf{h}]$, however, proved itself to be a necessary requirement for the analytical approach to be feasible. This clarifies the special status of the self dual points (4): they are the only points of the parameter space where this duality mapping leads to an analytic solution.

Here we develop a similar duality mapping for the calculation of the entanglement entropies, or, more precisely, of the traces of integer powers of the reduced density matrix $\rho_A(t)$. We will see that also $\text{tr}[(\rho_A(t))^n]$ can be written as the trace of a power of an appropriate transfer matrix in time. In Secs. V and VI we then show that, at the self dual points and for the special initial states (15) and (16), such a trace can be analytically evaluated.

Considering $\text{tr}[(\rho_A(t))^n]$ and using the definitions (12) and (13) we find

$$\begin{aligned} \text{tr}[(\rho_A(t))^n] = & \sum_{\{\mathbf{a}_i\}, \{\mathbf{b}_i\}} \langle \psi_{\theta, \phi} | (U_{\text{KI}}[\mathbf{h}])^{-t} | \mathbf{a}_1, \mathbf{b}_2 \rangle \langle \mathbf{a}_1, \mathbf{b}_1 | (U_{\text{KI}}[\mathbf{h}])^t | \psi_{\theta, \phi} \rangle \\ & \times \langle \psi_{\theta, \phi} | (U_{\text{KI}}[\mathbf{h}])^{-t} | \mathbf{a}_2, \mathbf{b}_3 \rangle \langle \mathbf{a}_2, \mathbf{b}_2 | (U_{\text{KI}}[\mathbf{h}])^t | \psi_{\theta, \phi} \rangle \\ & \vdots \\ & \times \langle \psi_{\theta, \phi} | (U_{\text{KI}}[\mathbf{h}])^{-t} | \mathbf{a}_n, \mathbf{b}_1 \rangle \langle \mathbf{a}_n, \mathbf{b}_n | (U_{\text{KI}}[\mathbf{h}])^t | \psi_{\theta, \phi} \rangle \end{aligned} \quad (27)$$

where $|\mathbf{a}_i, \mathbf{b}_j\rangle = |\mathbf{a}_i\rangle \otimes |\mathbf{b}_j\rangle$, $|\mathbf{a}_i\rangle \in \mathcal{B}_N$, $|\mathbf{b}_i\rangle \in \mathcal{B}_{L-N}$, for $i, j \in \{1, 2, \dots, n\}$. Here we denoted by \mathcal{B}_j the computational basis of

$$\mathcal{H}_j = (\mathbb{C}^2)^{\otimes j}. \quad (28)$$

An explicit expression of \mathcal{B}_j is obtained replacing L by j in the expression (7).

Eq. (27) allows one to interpret the trace of the n -th power of the reduced density matrix as the partition function of a classical statistical mechanical model on a

multi-sheeted two-dimensional lattice, see Fig. 4 for a pictorial representation in the case $n = 3$. To see it more explicitly we consider a single ‘‘building block’’

$$\langle \mathbf{a}, \mathbf{b} | (U_{\text{KI}}[\mathbf{h}])^t | \psi_{\theta, \phi} \rangle, \quad (29)$$

and show that it is equivalent to the partition function of a classical Ising model (with complex weights) on a $t \times L$ lattice with periodic boundary conditions in space and fixed boundary conditions in time. This is seen in two steps. First, we insert t resolutions of the identity operator in the basis (7) into (29), obtaining

$$\begin{aligned} \langle \mathbf{a}, \mathbf{b} | (U_{\text{KI}}[\mathbf{h}])^t | \psi_{\theta, \phi} \rangle = & \sum_{\{\mathbf{s}_\tau\}} \prod_{\tau=1}^{t-1} \langle \mathbf{s}_{\tau+1} | U_{\text{KI}}[\mathbf{h}] | \mathbf{s}_\tau \rangle \\ & \times \langle \mathbf{a}, \mathbf{b} | U_{\text{KI}}[\mathbf{h}] | \mathbf{s}_t \rangle \langle \mathbf{s}_1 | \psi_{\theta, \phi} \rangle. \end{aligned} \quad (30)$$

Then we evaluate the matrix elements

$$\langle \mathbf{s} | \psi_{\theta, \phi} \rangle = \prod_{j=1}^L [\cos(\theta_j/2) \delta_{s_j, 1} + \sin(\theta_j/2) e^{i\phi_j} \delta_{s_j, -1}], \quad (31)$$

and

$$\begin{aligned} \langle \mathbf{s} | U_{\text{KI}}[\mathbf{h}] | \mathbf{r} \rangle = & \left(\frac{i}{2} \right)^{\frac{L}{2}} \exp \left[-\frac{i\pi}{4} \sum_{j=1}^L s_j r_j \right] \\ & \times \exp \left[-\frac{i\pi}{4} \sum_{j=1}^L r_j r_{j+1} - i \sum_{j=1}^L h_j r_j \right], \end{aligned} \quad (32)$$

Here, to find the last equation we set $r_{L+1} = r_1$ and we used the identity

$$\langle s | e^{i\frac{\pi}{4}\sigma^x} | r \rangle = \sqrt{\frac{i}{2}} \exp \left[-i\frac{\pi}{4} sr \right], \quad s, r \in \{\pm 1\}, \quad (33)$$

to treat the ‘‘kick’’ part of the Floquet operator $U_{\text{KI}}[\mathbf{h}]$. Putting all together we have

$$\begin{aligned} \langle \mathbf{a}, \mathbf{b} | (U_{\text{KI}}[\mathbf{h}])^t | \psi_{\theta, \phi} \rangle = & \left(\frac{i}{2} \right)^{\frac{tL}{2}} \sum_{\{\mathbf{s}_{\tau,j}\}} \exp \left[-\frac{i\pi}{4} \sum_{\tau=1}^t \sum_{j=1}^L s_{\tau,j} s_{\tau,j+1} - \frac{i\pi}{4} \sum_{\tau=1}^{t-1} \sum_{j=1}^L s_{\tau,j} s_{\tau+1,j} - i \sum_{\tau=1}^t \sum_{j=1}^L h_j s_{\tau,j} \right] \\ & \times \exp \left[-\frac{i\pi}{4} \sum_{j=1}^N s_{t,j} a_j - \frac{i\pi}{4} \sum_{j=N+1}^L s_{t,j} b_{j-N} \right] \prod_{j=1}^L (\cos(\theta_j/2) \delta_{s_{1,j}, 1} + \sin(\theta_j/2) e^{i\phi_j} \delta_{s_{1,j}, -1}), \end{aligned} \quad (34)$$

which, as promised, is the partition function of the classical Ising model on a two-dimensional cylinder.

Representing in this way each of the $2n$ building blocks in (27) and summing over $\{\mathbf{a}_j, \mathbf{b}_j\}$, one connects together

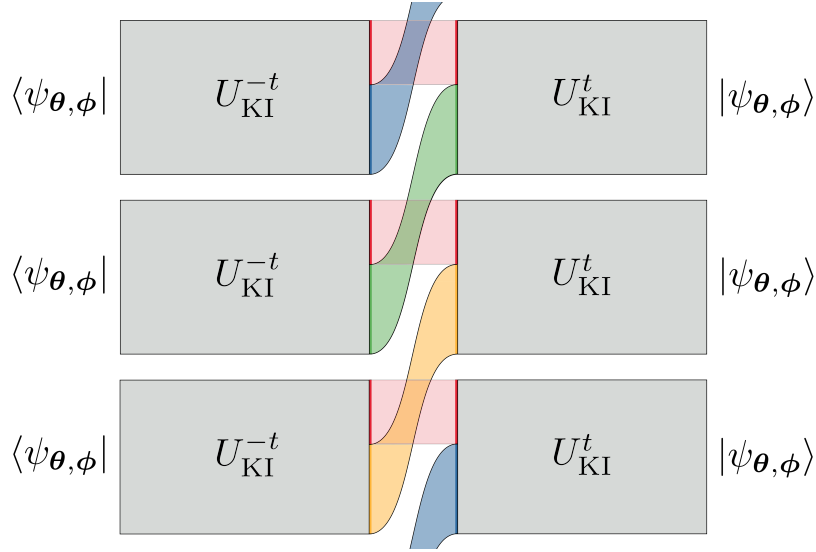


FIG. 4. Schematic representation of $\text{tr}[(\rho_A(t))^3]$ according to the expression (27). The six different cylinders corresponding to the partition functions (34) are schematically represented as rectangles. The spin subchains A and A^c connected with the coloured belts share identical spin configurations.

the $2n$ different cylinders obtaining the announced multi-sheeted lattice. Explicitly we have

$$\begin{aligned} \text{tr}[(\rho_A(t))^n] &= \frac{1}{2^{nLt}} \sum_{\{s_{\nu,\tau,j}\}} \exp \left[-i \sum_{j=1}^L \sum_{\nu=1}^{2n} \text{sgn}(n-\nu) \left(\sum_{\tau=1}^t \left(\frac{\pi}{4} s_{\nu,\tau,j} s_{\nu,\tau,j+1} + h_j s_{\nu,\tau,j} \right) + \sum_{\tau=1}^{t-1} \frac{\pi}{4} s_{\nu,\tau,j} s_{\nu,\tau+1,j} \right) \right] \\ &\times \prod_{\nu=1}^n \left\{ \prod_{j=1}^N (1 + s_{\nu,t,j} s_{\nu+n,t,j}) \prod_{j=N+1}^L (1 + s_{\nu,t,j} s_{n+1+\text{mod}(\nu-2,n),t,j}) \right\} \\ &\times \prod_{\nu=1}^{2n} \prod_{j=1}^L \left(\cos(\theta_j/2) \delta_{s_{\nu,1,j},1} + \sin(\theta_j/2) e^{i\phi_j \text{sgn}(n-\nu)} \delta_{s_{\nu,1,j},-1} \right), \end{aligned} \quad (35)$$

where $\text{sgn}(x)$ is the sign function (we adopted the convention $\text{sgn}(0) = 1$), $\text{mod}(m,n) = m \bmod n$ is the mod-function, and we introduced a new index $\nu \in \{1, 2, \dots, 2n\}$ such that strings $s_{\nu,\tau}$ with $\nu \leq n$ belong to terms in (27) with forward time evolution, while those with $\nu > n$ belong to terms in (27) with backward time evolution.

The second line of (35) is obtained by explicitly summing over $\{\mathbf{a}_i\}$ and $\{\mathbf{b}_i\}$ with the help of the identity

$$\sum_{a \in \{\pm 1\}} \exp \left[-i \frac{\pi}{4} a(s-r) \right] = 1 + sr, \quad s, r \in \{\pm 1\}. \quad (36)$$

We see that this line forces the configurations spins in the subchains A and A^c on the edges of different cylinders to be the same. These “frozen” configurations are represented by coloured strips in Fig. 4.

To proceed, it is useful to introduce the tensor product space $\mathcal{H}_t^{\otimes 2n}$, composed of $2n$ copies of \mathcal{H}_t , which is the space where the dual Floquet operator $\tilde{U}_{\text{KI}}[\tilde{\mathbf{h}}]$ acts. More formally

$$\mathcal{H}_t^{\otimes 2n} = \overbrace{\mathcal{H}_t \otimes \dots \otimes \mathcal{H}_t}^{2n} \cong \mathcal{H}_{2nt}. \quad (37)$$

Then, we define the operators $\mathbb{T}_{\theta,\phi}[h]$ and $\mathbb{R}_{\theta,\phi}[h]$ on $\mathcal{H}_t^{\otimes 2n}$ through their matrix elements in the computational basis

$$\begin{aligned} \langle \{s_{\nu,\tau}\} | \mathbb{T}_{\theta,\phi}[h] | \{r_{\nu,\tau}\} \rangle &= \frac{1}{2^{(t-1)n}} \exp \left[-i \sum_{\nu=1}^{2n} \text{sgn}(n-\nu) \left(\sum_{\tau=1}^t \left(\frac{\pi}{4} s_{\nu,\tau} r_{\nu,\tau} + h_j s_{\nu,\tau} \right) + \sum_{\tau=1}^{t-1} \frac{\pi}{4} s_{\nu,\tau} s_{\nu,\tau+1} \right) \right] \\ &\times \prod_{\nu=1}^n \left(\frac{1 + s_{\nu,t} s_{\nu+n,t}}{2} \right) \prod_{\nu=1}^{2n} \left(\cos(\theta/2) \delta_{s_{\nu,1},1} + \sin(\theta/2) e^{i\phi \text{sgn}(n-\nu)} \delta_{s_{\nu,1},-1} \right), \end{aligned} \quad (38)$$

and

$$\begin{aligned} \langle \{s_{\nu,\tau}\} | \mathbb{R}_{\theta,\phi}[h] | \{r_{\nu,\tau}\} \rangle &= \frac{1}{2^{(t-1)n}} \exp \left[-i \sum_{\nu=1}^{2n} \text{sgn}(n-\nu) \left(\sum_{\tau=1}^t \left(\frac{\pi}{4} s_{\nu,\tau} r_{\nu,\tau} + h_j s_{\nu,\tau} \right) + \sum_{\tau=1}^{t-1} \frac{\pi}{4} s_{\nu,\tau} s_{\nu,\tau+1} \right) \right] \\ &\times \prod_{\nu=1}^n \left(\frac{1 + s_{\nu,t} s_{n+1+\text{mod}(\nu-2,n),t}}{2} \right) \prod_{\nu=1}^{2n} \left(\cos(\theta/2) \delta_{s_{\nu,1},1} + \sin(\theta/2) e^{i\phi \text{sgn}(n-\nu)} \delta_{s_{\nu,1},-1} \right), \end{aligned} \quad (39)$$

where the first subscript labels spin variables in the different copies of \mathcal{H}_t composing $\mathcal{H}_t^{\otimes 2n}$.

Using the above matrix elements it is immediate to see that the expression (35) can directly be rewritten as a trace (on $\mathcal{H}_t^{\otimes 2n}$) of products of $\mathbb{T}_{\theta,\phi}[h]$ and $\mathbb{R}_{\theta,\phi}[h]$, namely

$$\text{tr} [(\rho_A(t))^n] = \text{tr} \left[\left(\prod_{j=1}^N \mathbb{T}_{\theta_j,\phi_j}[h_j] \right) \left(\prod_{j=N+1}^L \mathbb{R}_{\theta_j,\phi_j}[h_j] \right) \right], \quad (40)$$

where we defined on *ordered* product of non-commuting operators $\{\mathbb{O}_j\}$ as

$$\prod_{j=a}^b \mathbb{O}_j = \begin{cases} \mathbb{O}_a \cdots \mathbb{O}_b & \text{if } a \leq b \\ \mathbb{1} & \text{if } a > b \end{cases}. \quad (41)$$

The rewriting achieved by (40) is pictorially represented in Fig. 5, again in the case $n = 3$.

In upcoming analysis it will be useful to think of $\mathcal{H}_t^{\otimes 2n}$ as a tensor product of two copies of \mathcal{H}_{nt} , grouping together the first and the last n copies of \mathcal{H}_t , see Fig. 6. Namely we write each element of the basis of $\mathcal{H}_t^{\otimes 2n}$ in the following way

$$|\{s_{a,\tau}\}_{1 \leq a \leq 2n}^{1 \leq \tau \leq t}\rangle = |\{s_{a,\tau}\}_{1 \leq a \leq n}^{1 \leq \tau \leq t}\rangle \otimes |\{s_{a,\tau}\}_{n < a \leq 2n}^{n < \tau \leq t}\rangle. \quad (42)$$

We call these two copies of \mathcal{H}_{nt} the “positive-time” and “negative-time” spaces respectively, as the components of $\mathbb{T}_{\theta,\phi}[h]$ and $\mathbb{R}_{\theta,\phi}[h]$ acting on those spaces come from terms in (27) respectively propagating forward and backward in time.

It is useful to note that $\mathbb{T}_{\theta,\phi}[h]$ and $\mathbb{R}_{\theta,\phi}[h]$ are the same up to a cyclic permutation of the copies of \mathcal{H}_t composing the negative-time space (i.e. a cyclic permutation of the second row of Fig. 6), namely

$$\mathbb{R}_{\theta,\phi}[h] = \mathbb{P} \mathbb{T}_{\theta,\phi}[h] \mathbb{P}^\dagger, \quad (43)$$

where we defined

$$\mathbb{P} = \mathbb{1} \otimes \prod_{\nu=1}^n \prod_{\tau=1}^t P_{(\nu,\tau),(\nu-1,\tau)}. \quad (44)$$

Here $P_{(\nu,\tau),(\nu-1,\tau)}$ is an elementary transposition

$$P_{(\nu,\tau),(\nu',\tau')} = \frac{1}{2} \mathbb{1} + \frac{1}{2} \sum_{a \in \{x,y,z\}} \sigma_{\nu,\tau}^a \sigma_{\nu',\tau'}^a. \quad (45)$$

where $\nu, \nu' \in \{1, \dots, n\}$ and $\tau, \tau' \in \{1, \dots, t\}$. The matrix $\sigma_{\nu,\tau}^a$ acts as the Pauli matrix σ^a , $a \in \{x, y, z\}$, at the site $\tau = 1, \dots, t$ of the ν -th copy of \mathcal{H}_t in \mathcal{H}_{nt} , i.e.

$$[\sigma_{\nu,\tau}^a, \sigma_{\nu',\tau'}^b] = 2i \delta_{\nu,\nu'} \delta_{\tau,\tau'} \varepsilon^{abc} \sigma_{\nu,\tau}^c, \quad \sigma_{0,\tau}^a \equiv \sigma_{n,\tau}^a. \quad (46)$$

Note that the property $P_{(\nu,\tau),(\mu,\sigma)} = P_{(\nu,\tau),(\mu,\sigma)}^{-1}$ implies $\mathbb{P}^\dagger = \mathbb{P}^{-1}$.

Writing (38) in matrix form we have that the transfer matrix is a simple tensor product of single-copy transfer matrices

$$\mathbb{T}_{\theta,\phi}[h] = \prod_{\nu=1}^n \mathbb{T}_{\theta,\phi}^{(\nu)}[h]. \quad (47)$$

The matrix $\mathbb{T}_{\theta,\phi}^{(\nu)}[h]$ acts non-trivially only on the ν -th copy of \mathcal{H}_t in both the positive-time and negative-time spaces (ν -th column of Fig. 6), and it is explicitly written as

$$\mathbb{T}_{\theta,\phi}^{(\nu)}[h] = \mathbb{B}_{\nu,1}^z[\theta] \cdot \mathbb{G}_{\nu,t}^z \cdot \mathbb{U}_{\phi}^{(\nu)}[h], \quad (48)$$

where we introduced the Hermitian matrix $\mathbb{B}_{\nu,\tau}^a[\theta]$, the projector $\mathbb{G}_{\nu,\tau}^a$, and the unitary matrix $\mathbb{U}_{\phi}^{(\nu)}[h]$ defined as follows

$$\mathbb{B}_{\nu,\tau}^a[\theta] \equiv 2 [\cos(\theta/2) P_{\nu,\tau}^{a,+} + \sin(\theta/2) P_{\nu,\tau}^{a,-}]^{\otimes 2}, \quad (49)$$

$$\mathbb{G}_{\nu,\tau}^a \equiv \frac{1}{2} (\mathbb{1} + \sigma_{\nu,\tau}^a \otimes \sigma_{\nu,\tau}^a), \quad (50)$$

$$\mathbb{U}_{\phi}^{(\nu)}[h] \equiv U_{\nu,\phi} e^{-ihM_{\nu}^z} e^{i\frac{\pi}{4} M_{\nu}^x} \otimes U_{\nu,\phi}^* e^{ihM_{\nu}^z} e^{-i\frac{\pi}{4} M_{\nu}^x}, \quad (51)$$

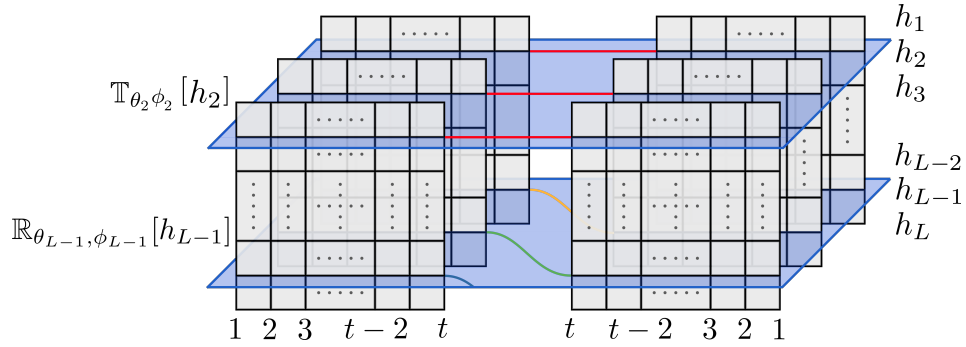


FIG. 5. Schematic depiction of $\text{tr}[(\rho_A(t))^3]$ written according to Eq. (40). Positive and negative time sheets are respectively on the left and on the right. Vertices connected by the coloured lines are coupled by the transfer matrices, in analogy with Fig. 4. Blue-shaded horizontal planes denote the spatial transfer matrices, specifically the operator $\mathbb{T}_{\theta, \phi}[h]$ for the physical sites corresponding to the block A of N spins, and the operator $\mathbb{R}_{\theta, \phi}[h] = \mathbb{P}\mathbb{T}_{\theta, \phi}[h]\mathbb{P}^\dagger$ for the sites corresponding to $L - N$ spins in A^c .

and finally

$$U_{\nu, \phi} \equiv \exp \left[-\frac{i\pi}{4} \sum_{\tau=1}^{t-1} \sigma_{\nu, \tau}^z \sigma_{\nu, \tau+1}^z - i\frac{\phi}{2} \sigma_{\nu, 1}^z \right], \quad (52)$$

$$M_\nu^a \equiv \sum_{\tau=1}^t \sigma_{\nu, \tau}^a, \quad (53)$$

$$P_{\nu, \tau}^{a, \pm} \equiv \frac{1}{2} (\mathbb{1} \pm \sigma_{\nu, \tau}^a). \quad (54)$$

Note that since

$$\left[\mathbb{T}_{\theta, \phi}^{(\nu)}[h], \mathbb{T}_{\theta, \phi}^{(\mu)}[h] \right] = 0, \quad \mu, \nu \in \{1, \dots, n\}, \quad (55)$$

the order in the product (47) is irrelevant. Putting everything together we have

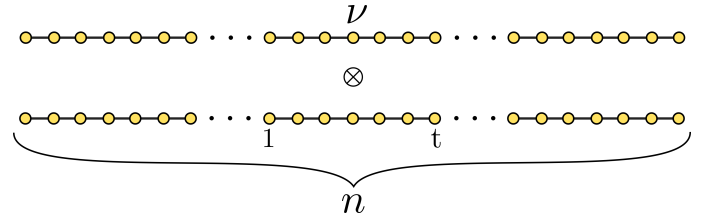


FIG. 6. Pictorial representation of the arrangement of the “dual” quantum spin degrees of freedom adopted in the tensor product space $\mathcal{H}_t^{\otimes 2n}$.

$$S_A^{(n)}(t) = \frac{1}{1-n} \log \text{tr} \left[\left(\prod_{j=1}^N \mathbb{T}_{\theta_j, \phi_j}[h_j] \right) \mathbb{P} \left(\prod_{j=N+1}^L \mathbb{T}_{\theta_j, \phi_j}[h_j] \right) \mathbb{P}^\dagger \right]. \quad (56)$$

This equation accomplishes the duality mapping of the entanglement entropies: we wrote the entanglement entropies in terms of the trace of products of an appropriate transfer matrix in space.

Before continuing with the evaluation of (56) two comments are in order. First we note that the mapping described can be performed also when J and b in (2) and (3) do not fulfil the self-duality condition (4). For generic J and b we obtain that the entropy is still given by (56) but the transfer matrix $\mathbb{T}_{\theta, \phi}[h]$ is modified in two ways. (i) the matrix $\mathbb{U}_\phi^{(\nu)}[h]$ is not unitary anymore. The Ising coupling in (52) replaced by \tilde{J} (cf. (25)) and the transverse fields in (51) (the coefficients of iM_ν^x in the positive and negative time copy) are respectively replaced by \tilde{b} and \tilde{b}^*

(cf. (26)). (ii) the projector $\mathbb{G}_{\nu, t}^z$ in (56) is replaced by

$$\cos \left(b \left(\sigma_{\nu, t}^z \otimes \mathbb{1} - \mathbb{1} \otimes \sigma_{\nu, t}^z \right) \right). \quad (57)$$

As we will see in the next section these changes are enough to hinder the analytical evaluation of (56), however, the duality approach can still be useful for perturbative calculations or numerical approaches.

We also observe that when the initial state is in the class \mathcal{L} (cf. (16)), namely when

$$\theta_j = \bar{\theta}_j \in \{0, \pi\}, \quad j \in \{1, 2, \dots, L\}, \quad (58)$$

the expression (56) can be further simplified by effectively reducing the dimension of the space where the trace acts. This is explicitly shown in Appendix B. The final result

is again of the form (56) with the replacement

$$\begin{aligned} \mathbb{T}_{\bar{\theta}_j, \phi_j}[h_j] &\longmapsto \bar{\mathbb{T}}_{\frac{\pi}{2}, \bar{\theta}_j - \frac{\pi}{2}}[h_j], \\ \mathbb{P} &\longmapsto \bar{\mathbb{P}}. \end{aligned} \quad (59)$$

Here the barred operators have exactly the same form as the non-barred ones (respectively (47) and (44)) but act on $\mathcal{H}_{t-1}^{\otimes 2n}$ instead of $\mathcal{H}_t^{\otimes 2n}$. Note that this is nothing but a restatement of Property (20).

V. SEPARATING STATES

Our goal is to use Equation (56) to determine $S_A^{(n)}(t)$ in the thermodynamic limit. To do that, however, we need some information on the Jordan normal form of the matrix $\mathbb{T}_{\theta, \phi}[h]$. Indeed, since the matrix is not normal, it is not guaranteed to be (and it is generically not) diagonalisable.

As proven in Appendix C, the form (47)–(48) of the transfer matrix has some simple but useful consequences on its Jordan normal form. Specifically we have

Property 1. *The following facts hold*

(i) $|\lambda_j| \leq \lambda_{\max} \equiv (1 + |\cos \theta|)^n, \forall \lambda_j \in \text{Spec}[\mathbb{T}_{\theta, \phi}[h]].$

(ii) *If an eigenvalue λ of $\mathbb{T}_{\theta, \phi}[h]$ fulfils $|\lambda| = \lambda_{\max}$ then*

- a. λ has trivial Jordan blocks (its geometric and algebraic multiplicities coincide).
- b. the associated left eigenvector $\langle A|$ satisfies

$$\langle A| \prod_{\nu=1}^n \mathbb{B}_{\nu, 1}^z[\theta] = \lambda_{\max} \langle A|, \quad (60)$$

$$\langle A| \prod_{\nu=1}^n \mathbb{G}_{\nu, t}^z = \langle A|, \quad (61)$$

$$\langle A| \prod_{\nu=1}^n \mathbb{U}_{\phi}^{(\nu)}[h] = e^{i\alpha} \langle A|, \quad \alpha \in \mathbb{R}, \quad (62)$$

where $\text{Spec}[A]$ denotes the spectrum of the matrix A .

Property 1 introduces the crucial simplification of this work. If the maximal eigenvalues of $\mathbb{T}_{\theta, \phi}[h]$ saturate the bounds at point (i) the problem of finding the maximal eigenvalues of the transfer matrix is *separated* into three much simpler ones, consisting of finding eigenvalues and eigenvectors of simple hermitian and unitary matrices.

The bound at point (i), however, cannot be always saturated. To see this, let us consider some constrains on the structure of the matrix $\mathbb{T}_{\theta, \phi}[h]$ coming from the identity (40). These are most easily found by considering the translational invariant case

$$h_j = h, \quad \theta_j = \theta, \quad \phi_j = \phi, \quad \forall j. \quad (63)$$

Setting $N = 0$ in (40) we have

$$\text{tr}[(\mathbb{T}_{\theta, \phi}[h])^L] = \text{tr}[(\rho(t))^n] = 1, \quad \forall L, n, \quad (64)$$

where in the second step we used that the state (12) is pure. This relation implies that the eigenvalues of $\mathbb{T}_{\theta, \phi}[h]$ are all 0 but one, which is equal to 1. Moreover, the Jordan block corresponding to the eigenvalue 1 is one-dimensional, while the eigenvalue 0 might have (and does have!) a highly nontrivial Jordan structure. More formally:

- (C1) $\text{Spec}[\mathbb{T}_{\theta, \phi}[h]] = \{0, 1\}.$
- (C2) The geometric multiplicity of the eigenvalue 1 is 1. (65)

From the conditions (65) it follows that the bound at point (i) of Property 1 can be saturated only when $\lambda_{\max} = 1$. Note that the cases for which $\lambda_{\max} = 1$ include $\theta = \pi/2$, but also $\theta = 0, \pi$. Indeed in the latter case the matrix $\mathbb{T}_{\theta, \phi}[h]$ can be replaced by $\bar{\mathbb{T}}_{\pi/2, \pi/2 - \theta}[h]$ (see (59) and Appendix B). In other words, the requirement $\lambda_{\max} = 1$ selects the two classes of states \mathcal{T} and \mathcal{L} introduced in Sec. III. This clarifies the meaning of their name. We called them “separating” states because if the initial state belongs to one of them the problem of finding the maximal eigenvalues of the transfer matrix (and the corresponding eigenvectors) can be separated. In the upcoming section we explicitly solve the separated problem (60)–(62) for $\lambda_{\max} = 1$, and, incidentally, we also verify that it has no solution for $\lambda_{\max} \neq 1$.

Finally, we note that away from the self dual points (4) the conditions (65) still hold and a property similar to Property 1 is still valid. In that case, however, the bound can never be saturated and no separation can be performed. This makes the problem analytically intractable, at least in an exact fashion.

VI. ENTANGLEMENT SPREADING FROM SEPARATING STATES

Here we explicitly solve the entanglement evolution from separating states. In particular in Sec. VIA we solve the separated problem (60)–(62) for $\lambda_{\max} = 1$ and in Sec. VIB we evaluate (56). To be concrete we focus on initial states in the class \mathcal{T} , the result for states in the class \mathcal{L} is obtained using (20).

A. Maximal eigenvalues of the transfer matrix

Our strategy is to determine the maximal eigenvalues of $\mathbb{T}_{\pi/2, \phi}[h]$ and the associated eigenvectors, by searching for all the vectors fulfilling (60)–(62) with $\lambda_{\max} = 1$. To simplify our analysis we make two observations. First we note that

$$\mathbb{B}_{\nu, 1}^z[\frac{\pi}{2}] = \mathbb{1} \otimes \mathbb{1}, \quad (66)$$

so that (60) becomes trivial for transverse separating states. Second, we note that all $\mathbb{G}_{\nu, t}^z$ and $\mathbb{U}_{\phi}^{(\nu)}$ commute

for different ν so we can look for simultaneous eigenvectors. The problem is then reduced to finding all vectors $\langle A |$ fulfilling

$$\langle A | \mathbb{G}_{\nu,t}^z = \langle A |, \quad (67)$$

$$\langle A | \mathbb{U}_{\phi}^{(\nu)} = \langle A | e^{i\alpha_{\nu}}, \quad \alpha_{\nu} \in \mathbb{R}, \quad \forall \nu \in \{1, \dots, n\}. \quad (68)$$

To solve these equations it is convenient to introduce the following one-to-one vector-to-operator mapping (*cf.* Ref. [55]) $\langle A | \leftrightarrow A$:

$$\langle A | = \sum_{k,m} \langle m | A | k \rangle \langle k | \otimes \langle m |^*, \quad (69)$$

where $\{|k\rangle\}$ is a basis of \mathcal{H}_{nt} and $(\cdot)^*$ denotes complex conjugation in the computational basis \mathcal{B}_{nt} , such that

$$\langle k |^* O^* | m \rangle^* = \langle k | O | m \rangle^*, \quad (70)$$

for any operator O . Using the mapping (69), Eqs. (67)–(68) are directly rewritten in operatorial form as follows

$$\sigma_{\nu,t}^z A = A \sigma_{\nu,t}^z, \quad (71)$$

$$U_{\nu,\phi} e^{-ihM_{\nu}^z} e^{i\frac{\pi}{4}M_{\nu}^x} A = e^{i\alpha_{\nu}} A U_{\nu,\phi} e^{-ihM_{\nu}^z} e^{i\frac{\pi}{4}M_{\nu}^x}, \quad (72)$$

for some $\alpha_{\nu} \in \mathbb{R}$ and all $\nu \in \{1, \dots, n\}$. In this formulation our goal is to find all independent linear operators A over \mathcal{H}_{nt} solving the commutation relations (71)–(72). As shown in Appendix D, these commutation relations are equivalent to

$$A \sigma_{\nu,\tau}^a = \sigma_{\nu,\tau}^a A, \quad (73)$$

for all $a \in \{x, y, z\}$, $\tau \in \{1, \dots, t\}$, $\nu \in \{1, \dots, n\}$. Namely, they are equivalent to requiring that A commutes with the entire algebra of observables in \mathcal{H}_{nt} . Since the latter is irreducible, Shur's Lemma implies that the unique (up to multiplicative factors) solution to (73) is given by

$$A = \mathbb{1}, \quad \text{and} \quad \alpha_{\nu} = 0. \quad (74)$$

We then find that the eigenvalue of $\mathbb{T}_{\pi/2,\phi}[h]$ with maximal magnitude is 1 and corresponds to the unique left eigenvector

$$\langle \mathbb{1} | = \frac{1}{2^{nt/2}} \sum_{\{s_{\nu,\tau}\}} \langle \{s_{\nu,\tau}\} | \otimes \langle \{s_{\nu,\tau}\} |, \quad (75)$$

$$\langle \Psi | \left(\prod_{j=1}^N \mathbb{T}_{\pi/4,\phi_j} [h_j] \right) | \Psi \rangle = \langle \Psi | \prod_{\nu=1}^n \left[\prod_{\tau=0}^{\lfloor \frac{N}{2} \rfloor - 1} [\mathbb{G}_{\nu,t-\tau}^z \mathbb{G}_{\nu,t-\tau}^x] [\mathbb{G}_{\nu,t-\lfloor \frac{N}{2} \rfloor}^z] \right]^{\text{mod}(N,2)} | \Psi \rangle, \quad \forall \phi_j, h_j, \quad (80)$$

where $\lfloor \cdot \rfloor$ denotes the floor function. We adopted the convention

$$\mathbb{G}_{\nu,\tau}^a = \mathbb{1}, \quad \tau \leq 0, \quad (81)$$

where we used the computational basis and omitted complex conjugation as the basis is real. Moreover, we included the normalisation factor $\sqrt{\text{tr}[\mathbb{1}]} = 2^{nt/2}$. Note that the unique right eigenvector of $\mathbb{T}_{\pi/2,\phi}[h]$ associated to $\lambda = 1$ is given by $|\mathbb{1}\rangle = (|\mathbb{1}\rangle)^{\dagger}$, as it can be directly verified.

We also observe that since we just proved that (61) and (62) have $\langle A | = \langle \mathbb{1} |$ as only solution, and, moreover

$$\langle \mathbb{1} | \prod_{\nu=1}^n \mathbb{B}_{\nu,1}^z[\theta] \neq \lambda_{\max} \langle \mathbb{1} |, \quad \theta \neq \pi/2, \quad (76)$$

the separated problem (60)–(62) has no solution for $\theta \neq \pi/2$.

B. Entanglement dynamics

Our next step is to use the eigenvectors determined above to compute the entanglement dynamics. First we note that the eigenvector $|\mathbb{1}\rangle$ is independent of ϕ and h . Moreover, $|\mathbb{1}\rangle$ is orthogonal to all left generalised eigenvectors corresponding to the eigenvalues 0 of $\mathbb{T}_{\pi/2,\phi}[h]$ for all ϕ and h . These two facts imply

$$\lim_{L \rightarrow \infty} S_A^{(n)}(t) = \frac{1}{1-n} \log \left[\langle \Psi | \left(\prod_{j=1}^N \mathbb{T}_{\pi/2,\phi_j} [h_j] \right) | \Psi \rangle \right], \quad (77)$$

where we introduced

$$|\Psi\rangle \equiv \mathbb{P}^{\dagger} |\mathbb{1}\rangle, \quad \langle \Psi | \equiv (|\Psi\rangle)^{\dagger} = \langle \mathbb{1} | \mathbb{P}. \quad (78)$$

The relation (77) can be used to find the slope of the linear growth of the entanglement entropy. Indeed, taking N to infinity we have

$$\lim_{N \rightarrow \infty} \lim_{L \rightarrow \infty} S_A^{(n)}(t) = \frac{2}{1-n} \log |\langle \Psi | \mathbb{1} \rangle| = 2t \log 2. \quad (79)$$

The simple structure of $\mathbb{T}_{\pi/2,\phi}[h]$, however, allows us to progress further and evaluate (77) exactly for each N . This can be done by making use of the following remarkable identity

and, to lighten the notation, here and in the following we assume that a product $\prod \dots$ only picks a single factor on

its right unless several terms are grouped within a square bracket $[\dots]$.

The identity (80) is proven in Appendix F using the explicit form of $\mathbb{T}_{\pi/2,\phi}[h]$ and the following useful properties of the state (78)

$$\prod_{\nu=1}^n O_\nu \otimes O_\nu^* |\Psi\rangle = |\Psi\rangle, \quad (82)$$

$$\langle\Psi| \prod_{\nu=1}^n O_\nu \otimes O_\nu^* = \langle\Psi|, \quad (83)$$

where O_ν acts non trivially, as the unitary operator O , only on the ν -th copy of \mathcal{H}_t in \mathcal{H}_{nt} , i.e. $O_\nu = \mathbb{1}_{\mathcal{H}_t}^{\otimes(\nu-1)} \otimes O \otimes \mathbb{1}_{\mathcal{H}_t}^{\otimes(n-\nu)}$. These properties are proven in Appendix E.

A striking consequence of (80) is that the entanglement entropies evolving from separating states are completely independent of the configuration of longitudinal magnetic fields $\{h_j\}$ and of the initial-state angles $\{\phi_i\}$. For instance, this means that the same result is obtained in the integrable and in the non-integrable case, with or without disorder.

The evaluation of the r.h.s. of (80) is now straightforward. First we note that in the computational basis (42) of $\mathcal{H}_t^{\otimes 2n}$ we have

$$\begin{aligned} & \langle\{s'_{\nu,\tau}\} \otimes \{r'_{\nu,\tau}\} | \prod_{\nu=1}^n \left[\prod_{\tau=0}^{\lfloor \frac{N}{2} \rfloor - 1} [\mathbb{G}_{\nu,t-\tau}^z \mathbb{G}_{\nu,t-\tau}^x] [\mathbb{G}_{\nu,t-\lfloor \frac{N}{2} \rfloor}^z]^{\text{mod}(N,2)} \right] |\{s_{\nu,\tau}\} \otimes |\{r_{\nu,\tau}\}\rangle \\ &= \begin{cases} \frac{1}{2^{n\lfloor \frac{N}{2} \rfloor}} \prod_{\nu=1}^n \left[\prod_{\tau=0}^{t-\lfloor \frac{N}{2} \rfloor} [\delta_{r'_{\nu,\tau} r_{\nu,\tau}} \delta_{s'_{\nu,\tau} s_{\nu,\tau}}] [\delta_{s_{\nu,t-\lfloor \frac{N}{2} \rfloor} r_{\nu,t-\lfloor \frac{N}{2} \rfloor}]^{\text{mod}(N,2)} \prod_{\tau=t-\lfloor \frac{N}{2} \rfloor+1}^t [\delta_{s_{\nu,\tau} r_{\nu,\tau}} \delta_{s'_{\nu,\tau} r'_{\nu,\tau}}] \right] & \lfloor \frac{N}{2} \rfloor < t \\ \frac{1}{2^{nt}} \prod_{\nu=1}^n \prod_{\tau=1}^t [\delta_{s_{\nu,\tau} r_{\nu,\tau}} \delta_{s'_{\nu,\tau} r'_{\nu,\tau}}] & \lfloor \frac{N}{2} \rfloor \geq t \end{cases}, \quad (84) \end{aligned}$$

where the matrix elements of $\mathbb{G}_{\nu,\tau}^x$ and $\mathbb{G}_{\nu,\tau}^z$ are computed by repeated use of

$$\begin{aligned} \langle s' | \otimes \langle r' | \mathbb{1} | s \rangle \otimes | r \rangle &= \delta_{s,s'} \delta_{r,r'}, \\ \langle s' | \otimes \langle r' | \frac{1}{2} (\mathbb{1} + \sigma^z \otimes \sigma^z) | s \rangle \otimes | r \rangle &= \delta_{s,s'} \delta_{r,r'} \delta_{s,r} = \delta_{s,s'} \delta_{s,r} \delta_{s',r'}, \\ \langle s' | \otimes \langle r' | \frac{1}{2} (\mathbb{1} + \sigma^z \otimes \sigma^z) \frac{1}{2} (\mathbb{1} + \sigma^x \otimes \sigma^x) | s \rangle \otimes | r \rangle &= \frac{1}{2} \delta_{s,r} \delta_{s',r'}, \quad s, r, s', r' \in \{\pm 1\}. \end{aligned} \quad (85)$$

Then, we plug (84) into the r.h.s. of Eq. (80). In particular, for $t > \lfloor N/2 \rfloor$ we find

$$\begin{aligned} & \langle\Psi| \prod_{\tau=0}^{\lfloor \frac{N}{2} \rfloor - 1} [\mathbb{G}_{\nu,t-\tau}^z \mathbb{G}_{\nu,t-\tau}^x] [\mathbb{G}_{\nu,t-\lfloor \frac{N}{2} \rfloor}^z]^{\text{mod}(N,2)} |\Psi\rangle = \\ &= \frac{1}{2^{n\lfloor \frac{N}{2} \rfloor + nt}} \sum_{\{s_{\nu,\tau}\}} \sum_{\{s'_{\nu,\tau}\}} \prod_{\nu=1}^n \left[\prod_{\tau=1}^{t-\lfloor \frac{N}{2} \rfloor} [\delta_{s'_{\nu+1,\tau} s_{\nu+1,\tau}} \delta_{s'_{\nu,\tau} s_{\nu,\tau}}] [\delta_{s_{\nu,t-\lfloor \frac{N}{2} \rfloor} s_{\nu+1,t-\lfloor \frac{N}{2} \rfloor}]^{\text{mod}(N,2)} \prod_{\tau=t-\lfloor \frac{N}{2} \rfloor+1}^t [\delta_{s_{\nu,\tau} s_{\nu+1,\tau}} \delta_{s'_{\nu,\tau} s'_{\nu+1,\tau}}] \right] \\ &= \frac{1}{2^{n\lfloor \frac{N}{2} \rfloor + nt}} \left[\sum_{\{s_{\nu,\tau}\}_{\tau < t-\lfloor \frac{N}{2} \rfloor}} 1 \right] \left[\sum_{\{s_{\nu,t-\lfloor \frac{N}{2} \rfloor}\}} [\delta_{s_{\nu,t-\lfloor \frac{N}{2} \rfloor} s_{\nu+1,t-\lfloor \frac{N}{2} \rfloor}]^{\text{mod}(N,2)} \right] \left[\sum_{\{s_{1,\tau}\}_{\tau > t-\lfloor \frac{N}{2} \rfloor}} 1 \right]^2 \\ &= \frac{1}{2^{n\lfloor \frac{N}{2} \rfloor + nt}} 2^{n(t-\lfloor \frac{N}{2} \rfloor-1)} 2^{n-(n-1)\text{mod}(N,2)} 2^{2\lfloor \frac{N}{2} \rfloor} = 2^{N(1-n)}. \end{aligned} \quad (86)$$

Proceeding analogously for $t \leq \lfloor N/2 \rfloor$ we have

$$\langle\Psi| \prod_{\tau=0}^{\lfloor \frac{N}{2} \rfloor - 1} [\mathbb{G}_{\nu,t-\tau}^z \mathbb{G}_{\nu,t-\tau}^x] [\mathbb{G}_{\nu,t-\lfloor \frac{N}{2} \rfloor}^z]^{\text{mod}(N,2)} |\Psi\rangle = 2^{2t(1-n)}. \quad (87)$$

Therefore, we finally obtain that for initial states in the class \mathcal{T} , all entanglement entropies are exactly given by Eq. (21).

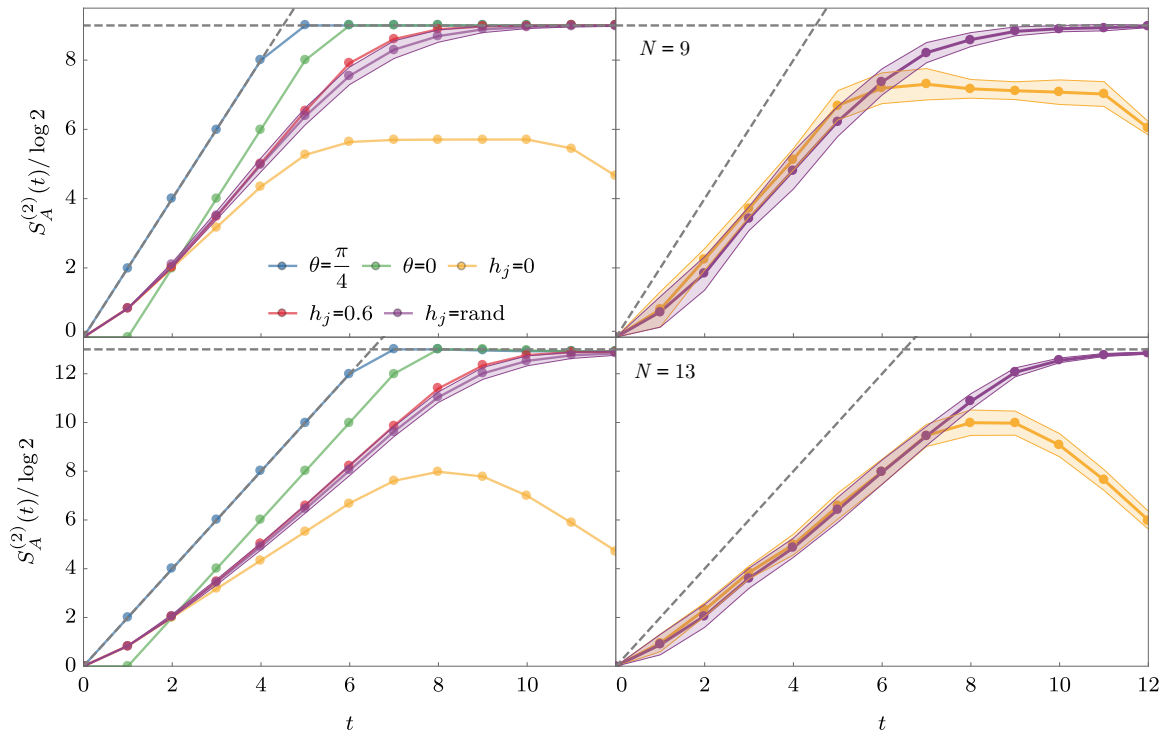


FIG. 7. The second Rényi entropy for a kicked Ising system of $L = 30$ spins evolving from “tilted” initial state (11). Top and bottom two panels have respectively $N = 9$ and $N = 13$. The two panels on the left report results for translational invariant initial states. The blue and green curves correspond respectively to transverse and longitudinal separating states (cf. (15) and (16)). Other curves correspond to the initial state $\theta_j = \phi_j = 1$ and different magnetic fields as indicated in the legend. The two panels on the right correspond to the maximally disordered cases, where the spins at each site point in a random direction and the magnetic fields h_j are either random (purple) or zero (yellow). In the cases with random parameters we show the average values for a sample of 8 realisations using a continuous line and indicate a standard deviation of one realisation by a shaded area.

VII. ENTANGLEMENT SPREADING FROM GENERIC STATES

Here, for completeness, we consider the entanglement spreading from generic product states (11) which are not separating. In this case we are unable to address the problem analytically and we resort to a numerical analysis. In principle, there are two complementary routes to do that: one can either numerically evaluate (14), which we call “direct route”, or (56), which we call “dual route” [66]. The former is more convenient to reach late times while the latter allows one to treat large systems. In particular, in the homogeneous case one can easily work in the thermodynamic limit using the dual route.

Since here we are interested in the scaling form of the entanglement entropies for large N and t we use the direct route. Specifically, we consider finite L and determine the time evolving state $|\psi_{\theta,\phi}(t)\rangle$, for $t \in \{0, 1, \dots, 12\}$, by means of the efficient direct-time propagation algorithm described in the supplemental material of Ref. [55]. The entanglement entropies are found

by computing and diagonalising the reduced density matrices $\rho_A(t)$ (cf. Eq. (13)) and using Eq. (14).

Some representative examples of our results are reported in Figs. 7 and 8. First of all we see that the qualitative behaviour is the same as before: the entropy grows in an approximately linear fashion until it saturates to a value proportional to the subsystem size. There are, however, a number of differences. First the evolution of the entropies appears to depend, although weakly for $\mathbf{h} \neq \mathbf{0}$, on the configuration of magnetic fields. Second entanglement entropies for different Rényi index n have a slightly different evolution, indicating a non-flat entanglement spectrum. Most importantly, however, a clear qualitative difference emerges between the integrable case, $\mathbf{h} = \mathbf{0}$, and the generic one. Indeed, while in the generic case the saturation value is independent of the initial state, in the integrable case it retains some memory of the initial state. Moreover, these two cases show very different finite size effects. In the integrable case the entropies start to decrease at times larger than $(L - N)/2$, while they remain at their maximal value in

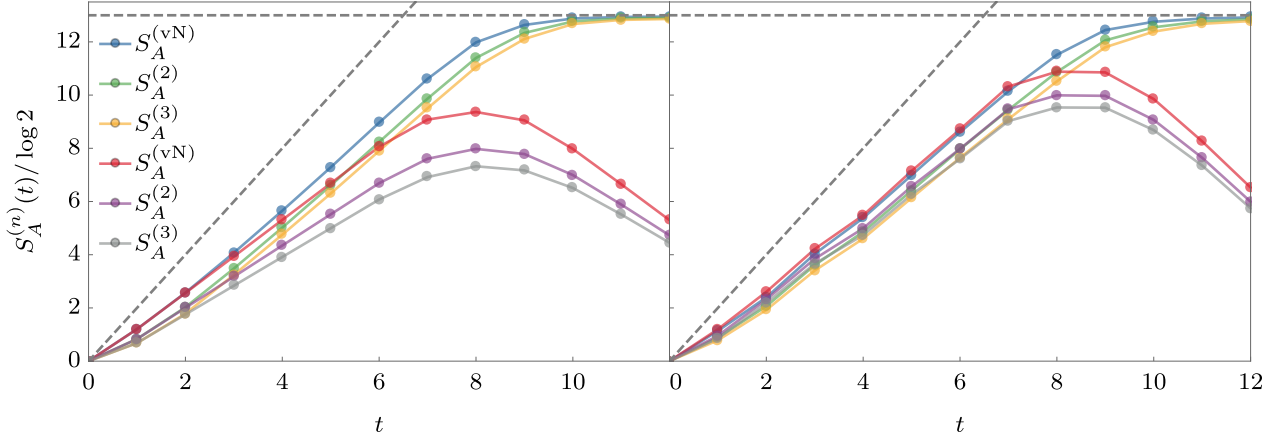


FIG. 8. Comparison of von Neumann, second and third Rényi entropies for a subsystem of $N = 13$ spins in a kicked Ising system of $L = 30$ spins. For generic initial states they are not equal, reflecting a non-trivial entanglement spectrum. In the left panel we fix $\theta_j = \phi_j = 1$ and $h_j = 0.6, 0$, whereas in the right we take the averages over 9 realisations and h_j are either random or 0. In both cases the red, purple and grey curves are for $\mathbf{h} = \mathbf{0}$.

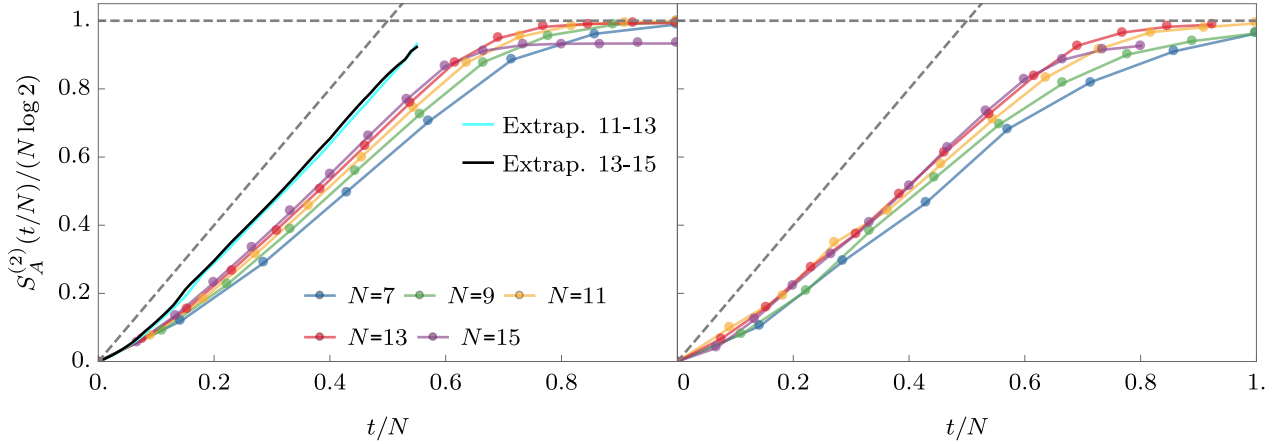


FIG. 9. Scaling form of the second Rényi entropy in a kicked Ising system of $L = 30$ spins. In the left panel we show the scaled form for different subsystem sizes and $h_j = 0.6$. For bigger system sizes the curves look more and more like the evolution from separating states. We also plot the curve resulting from simple linear extrapolation $1/N \rightarrow 0$ from datasets $N = 11, 13$ and $N = 13, 15$. The right panel shows the scaling form for the averages of 7 realisations of the maximally disordered case, where the spins at each site point in a random direction and magnetic fields h_j are also random. In the case $N = 15$ the correction for finite N/L [42, 67, 68] is clearly visible.

the non-integrable case. These behaviours respectively agree with the predictions of the quasiparticle and the minimal-membrane picture. Indeed, for finite L , the two pictures disagree also for our model. A more detailed discussion is presented in the following subsections.

A. Generic case

In the generic case the system always relaxes to the infinite temperature state, which is a hallmark of quantum ergodicity. Accordingly, the entropies are always observed to saturate to $N \log 2$ minus the expected correction due to a finite N/L [42, 67, 68]. The precise

functional form for how it does that is, however, harder to determine, as we cannot reach large enough systems. To determine at least the slope of the linear growth we considered the scaling form

$$\mathcal{S}^{(n)}(x) = \frac{S_A^{(n)}(x)}{N \log 2} \quad x \equiv t/N, \quad (88)$$

reported in Fig. 9 for $n = 2$. One can immediately note that the growth is faster for larger subsystem size. This makes us wonder whether in the limit of $t, N \rightarrow \infty$ and fixed x the slope goes to the maximal one as for separat-

ing states, namely whether

$$\lim_{\substack{t, N \rightarrow \infty \\ t/N = x}} \lim_{L \rightarrow \infty} \mathcal{S}^{(n)}(x) = \min(2x, 1). \quad (89)$$

To address this question we have performed a simple extrapolation to $1/N \rightarrow 0$, based on numerical data for the largest three accessible values of $N = 11, 13, 15$. The result, however, does not fall on the scaling curve (89). This could clearly be due to the fact that the system sizes considered are too small and the question remains open.

B. Integrable case

For $\mathbf{h} = \mathbf{0}$ the problem is integrable, or, more precisely, free. Indeed, it can be mapped to a problem of non-interacting Fermions via a combination of Jordan-Wigner and Bogoliubov transformations (see the supplemental material of [55]). This gives us the appealing opportunity of comparing our results with the quasiparticle picture of Ref. [15].

In the integrable case the Floquet Hamiltonian generating the time evolution can be explicitly computed for all values of J and b (see the supplemental material of [55]). In particular, at the self dual points it takes an especially simple form: the dispersion is exactly linear with unit slope. Surprisingly, however, the entanglement spreading from the states (11) cannot generically be solved analytically. Indeed, for generic values of θ and ϕ the states are not Gaussian in terms of the time evolving fermions. Moreover, since the dispersion is linear, the usual arguments about Gaussification do not apply [69, 70]. Interestingly, not even the separating states are always Gaussian: the states in \mathcal{T} are Gaussian only for $\phi_i = 0, \pi$.

In the inset of Fig. 10 we report the evolution of $S_A^{(2)}(t)$, computed numerically, for several homogeneous non-separating initial states characterised by different $\theta_j = \theta$ and $\phi_j = \phi$. We see that, in contrast with the generic case, the saturation value changes depending on θ and ϕ . This indicates that the system does not relax to the infinite temperature state but to a non-trivial generalised Gibbs ensemble retaining memory of the extensive number of local conserved charges of the system. Note that the density of free (Bogoliubov) fermions is independent of ϕ , so the ϕ -dependence of the plateau shows that the latter is not entirely fixed by such density. This is expected for non-Gaussian states.

Even if a full analytic treatment is out of reach, in the homogeneous case we can still find a prediction for the scaling form (88) by embracing the quasiparticle interpretation of Ref. [15]. To explain the finite-size effects observed in the numerics we consider the semiclassical prediction for large finite sizes L , which for convenience we take to be even. Using that the quasiparticles have all unit speed and assuming $N < L/2$ we find that $\mathcal{S}^{(n)}(x)$

is $L/2$ -periodic and for $x \in \{0, 1, \dots, L/2\}$ it reads as

$$\mathcal{S}^{(n)}(x) = \min\left(\min(2x, 1), \frac{L}{N} - 2x\right) S_{\theta, \phi}^{(n)}, \quad (90)$$

where $S_{\theta, \phi}^{(n)}$ is a (N - and L - independent) constant which cannot generically be determined for non-Gaussian states. As shown in the main panel of Fig. 10 this scaling form is in fair agreement with our numerical results already for $N = 11$.

VIII. CONCLUSIONS

We have developed a constructive and mathematically rigorous approach for computing the dynamics of bipartite entanglement in a class of “maximally scrambling”, locally interacting, chaotic spin chains. Specifically, we considered the so called “self-dual” kicked Ising spin chains, where the integrability is broken by switching on an external longitudinal magnetic field. We prepared the system in class of ground states of simple local Hamiltonians and determined exactly the dynamics of all Rényi entropies of finite blocks of spins of arbitrary size. The results presented are non-perturbative, no kind of averaging is involved, and, most importantly, they hold in the presence of longitudinal magnetic fields with arbitrary spatial dependence. It is remarkable that such an explicit exact calculation can be performed for a specific non-integrable many-body system.

Our result shows that in the thermodynamic limit the Rényi entropies of finite blocks of spins are independent of the longitudinal magnetic field at all times. Moreover, they obey universal scaling laws that can be predicted both by means of the quasiparticle picture of Ref. [15], put forward for integrable models, and of the minimal membrane picture of Ref. [49], propounded for generic systems. For finite systems, however, some qualitative differences emerge between the integrable and the non-integrable case. In particular we showed numerically that there are recurrences in the integrable case, which are absent in the non-integrable one. We stress that these differences are correctly accounted for by the quasiparticle and minimal membrane pictures, which disagree for finite sizes.

Our analytical method can be used to highlight qualitative differences in the entanglement spreading of integrable and non-integrable systems directly in the thermodynamic limit. To do that one could follow Refs. [35, 36] and consider the bipartite entanglement of disjoint blocks. Our preliminary results suggest that the scaling forms produced in the two cases are indeed different and respectively agree with the predictions of quasiparticle and membrane pictures. Another possible direction is to perturb the kicked Ising spin chains away from the “self-dual” points, where the predictions of the two pictures disagree also for the entanglement of a single block. This could be tested within our approach by using perturbation theory.

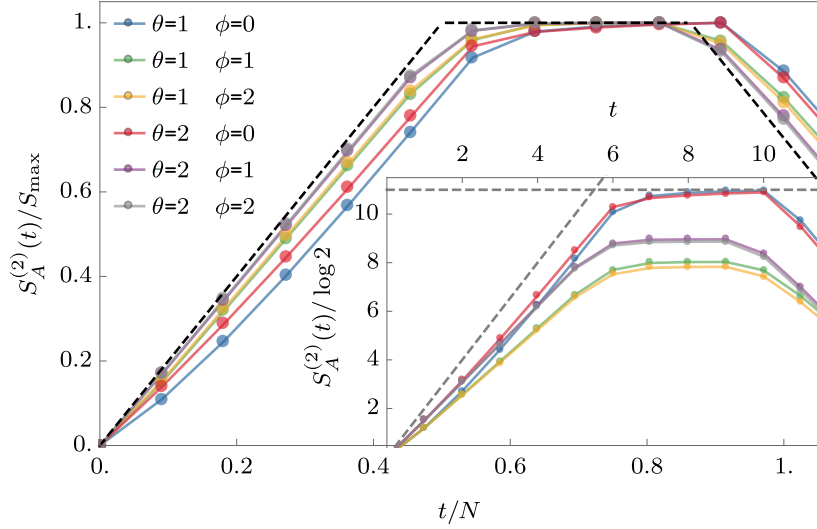


FIG. 10. The second Rényi entropy for a subsystem of $N = 11$ spins in a kicked Ising system of $L = 30$ at the integrable point $\mathbf{h} = 0$ for different translationally invariant initial states. In the main shows the rescaled curves, which are close to (90) (black dashed line), given by the quasiparticle picture. In the inset we show the non-rescaled version, where it is apparent that the saturation value depends on the initial state. Note a recurrence after the time $t = 10$, consistent with the quasiparticle picture.

More generally, we expect that our method would allow for explicit calculations similar to the ones presented also for other measures of correlations and dynamical complexity, such as operator space entanglement entropy and out-of-time order correlators.

Finally, we believe that the remarkable algebraic structure unveiled in this work paves the way for the determination of a new class of exactly solvable, maximally chaotic models. Elements of this class can serve as minimal models for characterising the non-equilibrium dynamics in generic systems.

ACKNOWLEDGEMENTS

We thank Adam Nahum for very valuable comments on the manuscript. B.B. and T.P. acknowledge the hospitality of the Erwin Schrödinger Institute (ESI), Vienna, where this project has been conceived. The work has been supported by Advanced Grant of European Research Council (ERC), No. 694544 – OMNES.

Appendix A: Duality of traces

Here we explicitly demonstrate the duality relation (24). Writing $\text{tr} \left[(U_{\text{KI}}[\mathbf{h}])^t \right]$ in the computational basis \mathcal{B}_L (cf. (7)) we have

$$\begin{aligned}
 \text{tr} \left[(U_{\text{KI}}[\mathbf{h}])^t \right] &= \sum_{\{\mathbf{s}_\tau\}} \langle \mathbf{s}_1 | U_{\text{KI}}[\mathbf{h}] | \mathbf{s}_t \rangle \langle \mathbf{s}_t | U_{\text{KI}}[\mathbf{h}] | \mathbf{s}_{t-1} \rangle \cdots \langle \mathbf{s}_2 | U_{\text{KI}}[\mathbf{h}] | \mathbf{s}_1 \rangle \\
 &= \left(\frac{\sin 2b}{2i} \right)^{\frac{Lt}{2}} \sum_{\{\mathbf{s}_{\tau,j}\}} \left\{ \exp \left[-i\tilde{J} \sum_{j=1}^L s_{1,j} s_{t,j} - iJ \sum_{j=1}^L s_{t,j} s_{t,j+1} - i \sum_{j=1}^L h_j s_{t,j} \right] \right. \\
 &\quad \times \exp \left[-i\tilde{J} \sum_{j=1}^L s_{t,j} s_{t-1,j} - iJ \sum_{j=1}^L s_{t-1,j} s_{t-1,j+1} - i \sum_{j=1}^L h_j s_{t-1,j} \right] \\
 &\quad \vdots \\
 &\quad \left. \times \exp \left[-i\tilde{J} \sum_{j=1}^L s_{2,j} s_{1,j} - iJ \sum_{j=1}^L s_{1,j} s_{1,j+1} - i \sum_{j=1}^L h_j s_{1,j} \right] \right\}. \tag{A1}
 \end{aligned}$$

Here $s_{\tau,L+j} \equiv s_{\tau,j}$ and in the second step we used the identity

$$\langle s | e^{-ib\sigma^x} | r \rangle = \sqrt{\frac{\sin 2b}{2i}} \exp \left[-i\tilde{J}sr \right], \quad s, r \in \{\pm 1\}, \quad (\text{A2})$$

where

$$\tilde{J} = -\frac{\pi}{4} - \frac{i}{2} \log \tan b. \quad (\text{A3})$$

This expression can be thought of as the partition function of a two-dimensional Ising model with complex couplings on a $L \times t$ periodic lattice. In other words, the r.h.s. of (A1) is proportional to the partition function of a classical statistical mechanical model with configuration energy given by

$$\mathcal{E}[\{s_{\tau,j}\}, \mathbf{h}] = - \sum_{\tau=1}^t \sum_{j=1}^L (iJ s_{\tau,j} s_{\tau,j+1} + i\tilde{J} s_{\tau,j} s_{\tau+1,j} + i h_j s_{\tau,j}). \quad (\text{A4})$$

Reorganising the sum on the r.h.s. of (A1) we also have

$$\begin{aligned} \text{tr} \left[(U_{\text{KI}}[\mathbf{h}])^t \right] &= \left(\frac{\sin 2b}{2i} \right)^{\frac{Lt}{2}} \sum_{\{s_{\tau,j}\}} \left\{ \exp \left[-i\tilde{J} \sum_{\tau=1}^t s_{\tau,1} s_{\tau+1,1} - iJ \sum_{\tau=1}^t s_{\tau,1} s_{\tau,L} - i \sum_{\tau=1}^t h_1 s_{\tau,1} \right] \right. \\ &\quad \times \exp \left[-i\tilde{J} \sum_{\tau=1}^t s_{\tau,2} s_{\tau+1,2} - iJ \sum_{\tau=1}^t s_{\tau,1} s_{\tau,2} - i \sum_{\tau=1}^t h_2 s_{\tau,2} \right] \\ &\quad \vdots \\ &\quad \left. \times \exp \left[-i\tilde{J} \sum_{\tau=1}^t s_{\tau,L} s_{\tau+1,L} - iJ \sum_{\tau=1}^t s_{\tau,L} s_{\tau,L-1} - i \sum_{\tau=1}^t h_L s_{\tau,L} \right] \right\}, \quad (\text{A5}) \end{aligned}$$

where we defined $s_{t+\tau,j} \equiv s_{\tau,j}$. Using again the identity (A2) we finally find

$$\text{tr} \left[(U_{\text{KI}}[\mathbf{h}])^t \right] = \text{tr} \left(\tilde{U}_{\text{KI}}[h_1 \tilde{\mathbf{1}}] \cdots \tilde{U}_{\text{KI}}[h_L \tilde{\mathbf{1}}] \right), \quad (\text{A6})$$

where ‘‘tilded’’ bold symbols denote vectors of t components and we introduced the dual transfer matrix

$$\tilde{U}_{\text{KI}}[\tilde{\mathbf{h}}] = e^{-i\tilde{H}_{\text{K}}} e^{-i\tilde{H}_{\text{I}}[\tilde{\mathbf{h}}]}, \quad (\text{A7})$$

with

$$\tilde{H}_{\text{I}}[\tilde{\mathbf{h}}] \equiv \tilde{J} \sum_{j=1}^t \sigma_j^z \sigma_{j+1}^z + \sum_{j=1}^t h_j \sigma_j^z, \quad \tilde{H}_{\text{K}} \equiv \tilde{b} \sum_{j=1}^t \sigma_j^x. \quad (\text{A8})$$

Appendix B: Simplified transfer matrix for longitudinal separating states

When the initial state is in the class \mathcal{L} (cf. (16)), namely when

$$\theta_j = \bar{\theta}_j \equiv (1 + s_j)\pi/2, \quad s_j \in \{-1, 1\}, \quad j \in \{1, 2, \dots, L\}, \quad (\text{B1})$$

the form (56) can be simplified by effectively reducing the dimension of the space where the trace acts. To see this we note that in this case $\mathbb{B}_{\nu,1}^z[\theta]$ becomes proportional to a projector:

$$\mathbb{B}_{\nu,1}^z[(1 + s_j)\pi/2] = 2P_{\nu,1}^{z,s_j} \otimes P_{\nu,1}^{z,s_j}, \quad (\text{B2})$$

so that we have

$$\begin{aligned} &\text{tr} \left[\left(\prod_{j=1}^N \mathbb{T}_{\bar{\theta}_j, \phi_j}[h_j] \right) \mathbb{P} \left(\prod_{j=N+1}^L \mathbb{T}_{\bar{\theta}_j, \phi_j}[h_j] \right) \mathbb{P}^\dagger \right] \\ &= 2^{Ln} \text{tr} \left[\prod_{j=1}^L \prod_{\nu=1}^n P_{\nu,1}^{z,s_j} e^{i\frac{\pi}{4}\sigma_{\nu,1}^x} \otimes P_{\nu,1}^{z,s_j} e^{-i\frac{\pi}{4}\sigma_{\nu,1}^x} \right] \text{tr} \left[\left(\prod_{j=1}^N \bar{\mathbb{T}}_{\frac{\pi}{2}, \bar{\theta}_j - \frac{\pi}{2}}[h_j] \right) \bar{\mathbb{P}} \left(\prod_{j=N+1}^L \bar{\mathbb{T}}_{\frac{\pi}{2}, \bar{\theta}_j - \frac{\pi}{2}}[h_j] \right) \bar{\mathbb{P}}^\dagger \right], \quad (\text{B3}) \end{aligned}$$

where we introduced

$$\bar{\mathbb{P}} \equiv \mathbb{1} \otimes \prod_{\nu=1}^n \prod_{\tau=2}^t P_{(\nu,\tau),(\nu-1,\tau)}, \quad (\text{B4})$$

$$\bar{\mathbb{T}}_{\theta,\phi}[h] \equiv \mathbb{B}_{\nu,2}^z[\theta] \cdot \mathbb{G}_{\nu,t}^z \cdot \bar{\mathbb{U}}_{\phi}[h]. \quad (\text{B5})$$

Here the matrix $\bar{\mathbb{U}}_{\phi}^{(\nu)}[h]$ is defined as

$$\bar{\mathbb{U}}_{\phi}^{(\nu)}[h] \equiv (\bar{U}_{\nu,\phi} \otimes \bar{U}_{\nu,\phi}^*) \cdot \left(e^{-ih\bar{M}_{\nu}^z} \otimes e^{ih\bar{M}_{\nu}^z} \right) \cdot \left(e^{i\frac{\pi}{4}\bar{M}_{\nu}^x} \otimes e^{-i\frac{\pi}{4}\bar{M}_{\nu}^x} \right), \quad (\text{B6})$$

and the barred operators read as

$$\bar{U}_{\nu,\phi} \equiv \exp \left[-\frac{i\pi}{4} \sum_{\tau=2}^{t-1} \sigma_{\nu,\tau}^z \sigma_{\nu,\tau+1}^z - i\frac{\phi}{2} \sigma_{\nu,2}^z \right], \quad \bar{M}_{\nu}^a \equiv \sum_{\tau=2}^t \sigma_{\nu,\tau}^a. \quad (\text{B7})$$

So they have the same form as (52) and (53) but at fixed ν they act non-trivially only in the space \mathcal{H}_{t-1} composed of the last $t-1$ sites of \mathcal{H}_t . In other words $\bar{\mathbb{T}}_{\theta,s}[h]$ has the same form as $\mathbb{T}_{\theta,s}[h]$ but acts on $\mathcal{H}_{t-1}^{\otimes 2n}$ instead of $\mathcal{H}_t^{\otimes 2n}$. We stress that the trace operations in expression (B3) and below are taken in the subspaces where the operators act nontrivially, for example, for the barred operators in $\mathcal{H}_{t-1}^{\otimes 2n} \cong \mathcal{H}_{2n(t-1)}$. Noting

$$2^{Ln} \text{tr} \left[\prod_{j=1}^L \prod_{\nu=1}^n P_{\nu,1}^{z,s_j} e^{i\frac{\pi}{4}\sigma_{\nu,1}^x} \otimes P_{\nu,1}^{z,s_j} e^{-i\frac{\pi}{4}\sigma_{\nu,1}^x} \right] = 2^{Ln} \left| \text{tr} \left[\prod_{j=1}^L \left[P_{1,1}^{z,s_j} e^{i\frac{\pi}{4}\sigma_{1,1}^x} \right] \right] \right|^{2n} = 1 \quad \forall s_j \in \{-1, +1\}, \quad (\text{B8})$$

we finally find

$$S_A^{(n)}(t) = \frac{1}{1-n} \log \text{tr} \left[\left(\prod_{j=1}^N \bar{\mathbb{T}}_{\frac{\pi}{2}, \bar{\theta}_j - \frac{\pi}{2}}[h_j] \right) \bar{\mathbb{P}} \left(\prod_{j=N+1}^L \bar{\mathbb{T}}_{\frac{\pi}{2}, \bar{\theta}_j - \frac{\pi}{2}}[h_j] \right) \bar{\mathbb{P}}^{\dagger} \right]. \quad (\text{B9})$$

Therefore we see that in this case the entropies are given by an expression of the form (56), with $\theta_j = \frac{\pi}{2}$ and $\phi_j = \frac{\pi}{2}s_j$, but with matrices acting on $\mathcal{H}_{t-1}^{\otimes 2n}$ instead of $\mathcal{H}_t^{\otimes 2n}$. Note that for $\theta_j = \bar{\theta}_j$ the states (11) do not depend on ϕ_i and this independence is correctly reflected in Eq. (B9).

Appendix C: Proof of Property 1

In this appendix we provide the proof of Property 1.

Proof. For each state $\langle A|$ we have

$$\langle A | \mathbb{T}_{\theta,\phi}[h] \mathbb{T}_{\theta,\phi}^{\dagger}[h] | A \rangle = \langle A | \prod_{\nu=1}^n \mathbb{B}_{\nu,1}^z[\theta] \prod_{\nu=1}^n \mathbb{G}_{\nu,t}^z \prod_{\nu=1}^n \mathbb{B}_{\nu,1}^z[\theta] | A \rangle \leq \langle A | \prod_{\nu=1}^n \mathbb{B}_{\nu,1}^z[\theta]^2 | A \rangle, \quad (\text{C1})$$

where we used that $\mathbb{G}_{\nu,t}^z$ is a projector, so its expectation value on a normalised state is smaller or equal to one. Expanding $\mathbb{B}_{\nu,1}^z[\theta]^2$ we then have

$$\begin{aligned} \langle A | \mathbb{T}_{\theta,\phi}[h] \mathbb{T}_{\theta,\phi}^{\dagger}[h] | A \rangle &\leq 4^n \langle A | \prod_{\nu=1}^n \left(\cos^4(\theta/2) P_{\nu,1}^{z,+} \otimes P_{\nu,1}^{z,+} + \sin^2(\theta/2) \cos^2(\theta/2) P_{\nu,1}^{z,-} \otimes P_{\nu,1}^{z,+} \right. \\ &\quad \left. + \sin^2(\theta/2) \cos^2(\theta/2) P_{\nu,1}^{z,+} \otimes P_{\nu,1}^{z,-} + \sin^4(\theta/2) P_{\nu,1}^{z,-} \otimes P_{\nu,1}^{z,-} \right) | A \rangle. \end{aligned} \quad (\text{C2})$$

Since $P_{\nu,1}^{z,\pm} \otimes P_{\nu,1}^{z,\pm}$ are orthogonal projectors we have

$$\langle A | \mathbb{T}_{\theta,\phi}[h] \mathbb{T}_{\theta,\phi}^{\dagger}[h] | A \rangle \leq 4^n \max(\sin^{4n}(\theta/2), \cos^{4n}(\theta/2)). \quad (\text{C3})$$

In particular, choosing $\langle A|$ to be the left eigenstate of $\mathbb{T}_{\theta,\phi}[h]$ corresponding to the eigenvalue λ we have

$$|\lambda| \leq 2^n \max(\sin^{2n}(\theta/2), \cos^{2n}(\theta/2)) = (1 + |\cos \theta|)^n = \lambda_{\max}, \quad (\text{C4})$$

which proves the first part of the claim.

To prove the point (ii) a. we proceed by *reductio ad absurdum*. Suppose that the Jordan block of λ is non-trivial: let $\langle A|$ be the eigenvector associated to λ and let $\langle B|$ be the first generalised eigenvector. As it is always possible, we choose $\langle B|$ to be normalised and orthogonal to $\langle A|$ (which is also normalised). We then have

$$\langle B| \mathbb{T}_{\theta,\phi}[h] = \lambda \langle B| + x \langle A| \quad x \neq 0. \quad (\text{C5})$$

This implies

$$\langle B| \mathbb{T}_{\theta,\phi}[h] \mathbb{T}_{\theta,\phi}^\dagger[h] |B\rangle = |\lambda_{\max}|^2 + |x|^2, \quad (\text{C6})$$

which is impossible because it contradicts (C3). Point (ii) b. follows by noting that in order to have the equality sign in (C3) we must have

$$\langle A| \prod_{\nu=1}^n \mathbb{B}_{\nu,1}^z[\theta] = \lambda_{\max} \langle A|, \quad (\text{C7})$$

$$\langle A| \prod_{\nu=1}^n \mathbb{G}_{\nu,t}^z = \langle A|. \quad (\text{C8})$$

Using now that $\langle A|$ is a left eigenvector of $\mathbb{T}_{\theta,\phi}[h]$ we have (62). This concludes the proof. \square

Appendix D: Simplified commutation relations

In this appendix we prove the following property.

Property 2. *The commutation relations (71)–(72) imply*

$$A \sigma_{\nu,\tau}^a = \sigma_{\nu,\tau}^a A, \quad \forall a \in \{x, y, z\}, \quad \tau \in \{1, \dots, t\}, \quad \nu \in \{1, \dots, n\}. \quad (\text{D1})$$

Proof. First of all we note that multiplying (72) on the left and on the right by $e^{-i\frac{\pi}{4}M_\nu^x} e^{ihM_\nu^z} U_{\nu,\phi}^\dagger$ we have

$$A e^{-i\frac{\pi}{4}M_\nu^x} e^{ihM_\nu^z} U_{\nu,\phi}^\dagger = e^{i\alpha_\nu} e^{-i\frac{\pi}{4}M_\nu^x} e^{ihM_\nu^z} U_{\nu,\phi}^\dagger A, \quad \alpha_\nu \in \mathbb{R}, \quad \forall \nu \in \{1, \dots, n\}. \quad (\text{D2})$$

Using the conditions (71), (72), and (D2) we see that A commutes with

$$e^{-i\frac{\pi}{4}M_\nu^x} e^{ihM_\nu^z} U_{\nu,\phi}^\dagger \sigma_{\nu,t}^z U_{\nu,\phi} e^{-ihM_\nu^z} e^{i\frac{\pi}{4}M_\nu^x} = e^{-i\frac{\pi}{4}M_\nu^x} \sigma_{\nu,t}^z e^{i\frac{\pi}{4}M_\nu^x} = -\sigma_{\nu,t}^y. \quad (\text{D3})$$

Indeed we have

$$\begin{aligned} & A e^{-i\frac{\pi}{4}M_\nu^x} e^{ihM_\nu^z} U_{\nu,\phi}^\dagger \sigma_{\nu,t}^z U_{\nu,\phi} e^{-ihM_\nu^z} e^{i\frac{\pi}{4}M_\nu^x} = \\ & e^{i\alpha_\nu} e^{-i\frac{\pi}{4}M_\nu^x} e^{ihM_\nu^z} U_{\nu,\phi}^\dagger A \sigma_{\nu,t}^z U_{\nu,\phi} e^{-ihM_\nu^z} e^{i\frac{\pi}{4}M_\nu^x} = \\ & e^{i\alpha_\nu} e^{-i\frac{\pi}{4}M_\nu^x} e^{ihM_\nu^z} U_{\nu,\phi}^\dagger \sigma_{\nu,t}^z A U_{\nu,\phi} e^{-ihM_\nu^z} e^{i\frac{\pi}{4}M_\nu^x} = \\ & e^{-i\frac{\pi}{4}M_\nu^x} e^{ihM_\nu^z} U_{\nu,\phi}^\dagger \sigma_{\nu,t}^z U_{\nu,\phi} e^{-ihM_\nu^z} e^{i\frac{\pi}{4}M_\nu^x} A, \end{aligned} \quad (\text{D4})$$

where in the first step we used (D2), in the second (72), and in the third (71). Using (71) we then have that A also commutes with

$$-i \sigma_{\nu,t}^y \sigma_{\nu,t}^z = \sigma_{\nu,t}^x. \quad (\text{D5})$$

We then have

$$[A, \sigma_{\nu,t}^a] = 0, \quad \forall a \in \{x, y, z\}, \quad \nu \in \{1, \dots, n\}. \quad (\text{D6})$$

Using (D6), (72), and (D2) we can then conclude the proof by induction.

We will prove that if

$$[A, \sigma_{\nu, \tau}^a] = 0, \quad \forall a \in \{x, y, z\}, \quad \tau \in \{\bar{\tau} + 1, \bar{\tau} + 2, \dots, t\}, \quad (\text{D7})$$

then

$$[A, \sigma_{\nu, \bar{\tau}}^a] = 0, \quad \forall a \in \{x, y, z\}, \quad (\text{D8})$$

and then proceeding by induction in $\bar{\tau} = t - 1, \dots, 1$. The basis of the induction is given by (D6), so we just need to prove the inductive step. Assuming (D7) and proceeding as in (D4) we can show that A commutes also with

$$\begin{aligned} & U_{\nu, \phi} e^{-ihM_{\nu}^z} e^{i\frac{\pi}{4}M_{\nu}^x} \left(\prod_{\tau=\bar{\tau}+1}^t \sigma_{\nu, \tau}^x \right) e^{-i\frac{\pi}{4}M_{\nu}^x} e^{ihM_{\nu}^z} U_{\nu, \phi}^{\dagger} \\ &= \left(\prod_{\tau=\bar{\tau}+1}^t -i\sigma_{\nu, \tau-1}^z \sigma_{\nu, \tau}^z e^{i2h\sigma_{\nu, \tau}^z} \sigma_{\nu, \tau}^x \right) = -i^{t-\bar{\tau}} \sigma_{\nu, \bar{\tau}}^z \sigma_{\nu, t}^z \left(\prod_{j=\bar{\tau}+1}^t e^{i2h\sigma_{\nu, j}^z} \sigma_{\nu, j}^x \right). \end{aligned} \quad (\text{D9})$$

The inductive hypothesis (D7) then implies

$$[A, \sigma_{\nu, \bar{\tau}}^z] = 0. \quad (\text{D10})$$

Reasoning now as in (D4) we then have that A also commutes with

$$e^{-i\frac{\pi}{4}M_{\nu}^x} e^{ihM_{\nu}^z} U_{\nu, \phi}^{\dagger} \sigma_{\nu, \bar{\tau}}^z U_{\nu, \phi} e^{-ihM_{\nu}^z} e^{i\frac{\pi}{4}M_{\nu}^x} = e^{-i\frac{\pi}{4}M_{\nu}^x} \sigma_{\nu, \bar{\tau}}^z e^{i\frac{\pi}{4}M_{\nu}^x} = -\sigma_{\nu, \bar{\tau}}^y, \quad (\text{D11})$$

$$e^{-i\frac{\pi}{4}M_{\nu}^x} e^{ihM_{\nu}^z} U_{\nu, \phi}^{\dagger} \sigma_{\nu, \bar{\tau}}^z U_{\nu, \phi} e^{-ihM_{\nu}^z} e^{i\frac{\pi}{4}M_{\nu}^x} \sigma_{\nu, \bar{\tau}}^z = e^{-i\frac{\pi}{4}M_{\nu}^x} \sigma_{\nu, \bar{\tau}}^z e^{i\frac{\pi}{4}M_{\nu}^x} \sigma_{\nu, \bar{\tau}}^z = -i\sigma_{\nu, \bar{\tau}}^x. \quad (\text{D12})$$

So we have

$$[A, \sigma_{\nu, \tau}^a] = 0, \quad a \in \{x, y, z\}, \quad \tau \in \{1, \dots, t\}, \quad \nu \in \{1, \dots, n\}. \quad (\text{D13})$$

This concludes the proof. \square

Appendix E: Proof of Eqs. (82) and (83)

Let us start by proving (82). First we note

$$\prod_{\nu=1}^n O_{\nu} \otimes O_{\nu}^* |\mathbb{1}\rangle = |\mathbb{1}\rangle. \quad (\text{E1})$$

This is explicitly proven as follows

$$\begin{aligned} \prod_{\nu=1}^n O_{\nu} \otimes O_{\nu}^* |\mathbb{1}\rangle &= \frac{1}{2^{nt/2}} \sum_{k, m, m'} \langle m | \prod_{\nu=1}^n O_{\nu} | k \rangle \langle m' | \prod_{\nu=1}^n O_{\nu} | k \rangle^* | m \rangle \otimes | m' \rangle^* \\ &= \frac{1}{2^{nt/2}} \sum_{m, m'} \langle m | \prod_{\nu=1}^n O_{\nu} O_{\nu}^{\dagger} | m' \rangle | m \rangle \otimes | m' \rangle^* = \frac{1}{2^{nt/2}} \sum_m | m \rangle \otimes | m \rangle^* = |\mathbb{1}\rangle. \end{aligned} \quad (\text{E2})$$

Here we used (70) and the fact that O_{ν} is unitary. Second, we observe that from the definition of O_{ν} it directly follows

$$\mathbb{P} \left(\prod_{\nu=1}^n O_{\nu} \otimes O_{\nu}^* \right) \mathbb{P}^{\dagger} = \prod_{\nu=1}^n O_{\nu} \otimes O_{\nu}^*. \quad (\text{E3})$$

Combining (E3) and (E1) we then have

$$\prod_{\nu=1}^n O_{\nu} \otimes O_{\nu}^* |\Psi\rangle = \prod_{\nu=1}^n O_{\nu} \otimes O_{\nu}^* \mathbb{P} |\mathbb{1}\rangle = \mathbb{P} \prod_{\nu=1}^n O_{\nu} \otimes O_{\nu}^* |\mathbb{1}\rangle = |\Psi\rangle. \quad (\text{E4})$$

So we proved (82) for any O_{ν} acting non trivially, as the unitary operator O , only on the ν -th copy of \mathcal{H}_t in \mathcal{H}_{nt} . The relation (83) follows immediately by taking the adjoint of

$$\prod_{\nu=1}^n O_{\nu}^{\dagger} \otimes O_{\nu}^{\dagger*} |\Psi\rangle = |\Psi\rangle. \quad (\text{E5})$$

Appendix F: Proof of Property (80)

In this appendix we prove Eq (80).

Proof. Defining

$$\mathbb{J}_{\nu,\tau} = \exp \left[-i\frac{\pi}{4}\sigma_{\nu,\tau+1}^z \sigma_{\nu,\tau}^z \right] \otimes \exp \left[i\frac{\pi}{4}\sigma_{\nu,\tau+1}^z \sigma_{\nu,\tau}^z \right] \quad \tau \in \{1, \dots, t-1\}, \quad \mathbb{J}_{\nu,\tau} = \mathbb{1} \quad \tau \leq 0, \quad (\text{F1})$$

$$\mathbb{Z}_{\nu,\tau}^h = \exp \left[-ih\sigma_{\nu,\tau}^z \right] \otimes \exp \left[ih\sigma_{\nu,\tau}^z \right] \quad \tau \in \{1, \dots, t\}, \quad \mathbb{Z}_{\nu,\tau}^h = \mathbb{1} \quad \tau \leq 0, \quad (\text{F2})$$

$$\mathbb{X}_{\nu,\tau} = \exp \left[i\frac{\pi}{4}\sigma_{\nu,\tau}^x \right] \otimes \exp \left[-i\frac{\pi}{4}\sigma_{\nu,\tau}^x \right] \quad \tau \in \{1, \dots, t\}, \quad \mathbb{X}_{\nu,\tau} = \mathbb{1} \quad \tau \leq 0, \quad (\text{F3})$$

we can rewrite the l.h.s. of (80) as follows

$$\langle \Psi | \prod_{j=1}^N \mathbb{T}_{\frac{\pi}{2}, \phi_j} [h_j] | \Psi \rangle = \langle \Psi | \prod_{\nu=1}^n \left[\prod_{j=1}^N \left(\mathbb{G}_{\nu,t}^z \mathbb{Z}_{\nu,1}^{\phi_j/2} \prod_{\tau=1}^{t-1} \mathbb{J}_{\nu,\tau} \prod_{\tau=1}^t \mathbb{Z}_{\nu,\tau}^h \prod_{\tau=1}^t \mathbb{X}_{\nu,\tau} \right) \right] | \Psi \rangle. \quad (\text{F4})$$

To simplify this expression we proceed as follows. First we commute every possible $\mathbb{J}_{\nu,\tau}, \mathbb{Z}_{\nu,\tau}, \mathbb{X}_{\nu,\tau}$ to the left by using the following commutation relations

$$\mathbb{J}_{\nu,\tau} \mathbb{Z}_{\nu,\tau'}^h = \mathbb{Z}_{\nu,\tau'}^h \mathbb{J}_{\nu,\tau} \quad \forall \tau, \tau', \quad (\text{F5})$$

$$\mathbb{J}_{\nu,\tau} \mathbb{X}_{\nu,\tau'} = \mathbb{X}_{\nu,\tau'} \mathbb{J}_{\nu,\tau} \quad \tau' \neq \tau, \tau + 1, \quad (\text{F6})$$

$$\mathbb{X}_{\nu,\tau} \mathbb{Z}_{\nu,\tau'}^h = \mathbb{Z}_{\nu,\tau'}^h \mathbb{X}_{\nu,\tau} \quad \tau' \neq \tau, \quad (\text{F7})$$

$$\mathbb{J}_{\nu,\tau} \mathbb{G}_{\nu,\tau'}^z = \mathbb{G}_{\nu,\tau'}^z \mathbb{J}_{\nu,\tau} \quad \forall \tau', \tau, \quad (\text{F8})$$

$$\mathbb{Z}_{\nu,\tau}^h \mathbb{G}_{\nu,\tau'}^z = \mathbb{G}_{\nu,\tau'}^z \mathbb{Z}_{\nu,\tau}^h \quad \forall \tau', \tau, \quad (\text{F9})$$

$$\mathbb{X}_{\nu,\tau} \mathbb{G}_{\nu,\tau'}^z = \mathbb{G}_{\nu,\tau'}^z \mathbb{X}_{\nu,\tau} \quad \tau' \neq \tau. \quad (\text{F10})$$

Then we use

$$\langle \Psi | \prod_{\nu=1}^n \mathbb{J}_{\nu,\tau} = \langle \Psi |, \quad (\text{F11})$$

$$\langle \Psi | \prod_{\nu=1}^n \mathbb{X}_{\nu,\tau'} = \langle \Psi |, \quad (\text{F12})$$

$$\langle \Psi | \prod_{\nu=1}^n \mathbb{Z}_{\nu,\tau'}^h = \langle \Psi |, \quad (\text{F13})$$

which follow from (82). Finally, using also

$$\prod_{\nu=1}^n \mathbb{J}_{\nu,\tau} | \Psi \rangle = | \Psi \rangle, \quad (\text{F14})$$

$$\prod_{\nu=1}^n \mathbb{X}_{\nu,\tau'} | \Psi \rangle = | \Psi \rangle, \quad (\text{F15})$$

$$\prod_{\nu=1}^n \mathbb{Z}_{\nu,\tau'}^h | \Psi \rangle = | \Psi \rangle, \quad (\text{F16})$$

following from (83), on the rightmost term in the product over j we find

$$\langle \Psi | \prod_{j=1}^N \mathbb{T}_{\frac{\pi}{4}, \phi_j} [h_j] | \Psi \rangle = \langle \Psi | \prod_{\nu=1}^n \left[\prod_{j=1}^{N-1} \mathbb{A}_{\nu,j} \right] | \Psi \rangle, \quad (\text{F17})$$

where we defined

$$\mathbb{A}_{\nu,j} = \mathbb{G}_{\nu,t}^z \prod_{\tau=t-j+1}^{t-1} \mathbb{J}_{\nu,\tau} \prod_{\tau=t-j+2}^t \tilde{\mathbb{Z}}_{\nu,\tau}^{h_j, \phi_j} \prod_{\tau=t-j+1}^t \mathbb{X}_{\nu,\tau} \mathbb{G}_{\nu,t}^z, \quad (\text{F18})$$

$$\tilde{\mathbb{Z}}_{\nu,\tau}^{h,\phi} = \mathbb{Z}_{\nu,\tau}^{h+(\phi/2)\delta_{\tau,1}}. \quad (\text{F19})$$

Using

$$\begin{aligned} \mathbb{G}_{\nu,\tau}^z \mathbb{X}_{\nu,\tau} \mathbb{G}_{\nu,\tau}^z &= \mathbb{G}_{\nu,\tau}^z \left[\mathbb{G}_{\nu,\tau}^x + \frac{i}{2} [\sigma_{\nu,\tau}^x \otimes \mathbb{1} - \mathbb{1} \otimes \sigma_{\nu,\tau}^x] \right] \mathbb{G}_{\nu,\tau}^z \\ &= \mathbb{G}_{\nu,\tau}^z \left[\mathbb{G}_{\nu,\tau}^x \mathbb{G}_{\nu,\tau}^x + \frac{i}{4} [\mathbb{1} - \sigma_{\nu,\tau}^z \otimes \sigma_{\nu,\tau}^z] [\sigma_{\nu,\tau}^x \otimes \mathbb{1} - \mathbb{1} \otimes \sigma_{\nu,\tau}^x] \right] \\ &= \mathbb{G}_{\nu,\tau}^z \mathbb{G}_{\nu,\tau}^x \mathbb{G}_{\nu,\tau}^z = \mathbb{G}_{\nu,\tau}^z \mathbb{G}_{\nu,\tau}^x, \end{aligned} \quad (\text{F20})$$

we can rewrite (F18) as follows

$$\mathbb{A}_{\nu,j} = \mathbb{G}_{\nu,t}^z \mathbb{J}_{\nu,t-1} \mathbb{G}_{\nu,t}^x \prod_{\tau=t-j+1}^{t-2} \mathbb{J}_{\nu,\tau} \prod_{\tau=t-j+2}^{t-1} \tilde{\mathbb{Z}}_{\nu,\tau}^{h_j, \phi_j} \prod_{\tau=t-j+1}^{t-1} \mathbb{X}_{\nu,\tau}. \quad (\text{F21})$$

We now make use the following Lemma, proven in Appendix F1, to simplify the products of $\mathbb{A}_{\nu,j}$ s

Lemma 1.

$$\mathbb{A}_{\nu,1} \cdots \mathbb{A}_{\nu,2n} = \mathbb{J}_{\nu,t-1} \prod_{j=0}^{n-1} [\mathbb{G}_{\nu,t-j}^z \mathbb{G}_{\nu,t-j}^x] \mathbb{G}_{\nu,t-n}^z \mathbb{X}_{\nu,t-n} \prod_{j=n}^{2n-2} \left[\prod_{\tau=t-1-j}^{t-2n+j} \mathbb{J}_{\nu,\tau} \prod_{\tau=t-j}^{t-2n+j} \tilde{\mathbb{Z}}_{\nu,\tau}^{h_{j+2}, \phi_{j+2}} \prod_{\tau=t-1-j}^{t-2n+j+1} \mathbb{X}_{\nu,\tau} \right], \quad (\text{F22})$$

$$\mathbb{A}_{\nu,1} \cdots \mathbb{A}_{\nu,2n+1} = \mathbb{J}_{\nu,t-1} \prod_{j=0}^n [\mathbb{G}_{\nu,t-j}^z \mathbb{G}_{\nu,t-j}^x] \prod_{j=n}^{2n-1} \left[\prod_{\tau=t-1-j}^{t-2n-1+j} \mathbb{J}_{\nu,\tau} \prod_{\tau=t-j}^{t-2n+j-1} \tilde{\mathbb{Z}}_{\nu,\tau}^{h_{j+2}, \phi_{j+2}} \prod_{\tau=t-1-j}^{t-2n+j} \mathbb{X}_{\nu,\tau} \right], \quad n \geq 1. \quad (\text{F23})$$

Using now (F11), (F14), (F15), and (F16) we have

$$\langle \Psi | \prod_{j=1}^N \mathbb{T}_{\frac{\pi}{4}, \phi_j} [h_j] | \Psi \rangle = \langle \Psi | \prod_{\nu=1}^n \left[\prod_{j=0}^{\lfloor \frac{N}{2} \rfloor - 1} [\mathbb{G}_{\nu,t-j}^z \mathbb{G}_{\nu,t-j}^x] [\mathbb{G}_{\nu,t-\lfloor N/2 \rfloor}^z]^{\text{mod}(N,2)} \right] | \Psi \rangle, \quad (\text{F24})$$

which concludes the proof. \square

1. Proof of Lemma 1.

Here we prove Lemma 1.

Proof. We proceed by induction in the number of terms in the products of $\mathbb{A}_{\nu,j}$ s. First we establish the basis. We begin by computing

$$\begin{aligned} \mathbb{A}_{\nu,1} \mathbb{A}_{\nu,2} &= \mathbb{G}_{\nu,t}^z \mathbb{J}_{\nu,t-1} \mathbb{G}_{\nu,t}^x \mathbb{G}_{\nu,t}^z \mathbb{J}_{\nu,t-1} \mathbb{G}_{\nu,t}^x \mathbb{X}_{\nu,t-1} \\ &= \mathbb{J}_{\nu,t-1} \mathbb{G}_{\nu,t}^z \mathbb{G}_{\nu,t}^x \mathbb{G}_{\nu,t-1}^z \mathbb{X}_{\nu,t-1}. \end{aligned} \quad (\text{F25})$$

where we used

$$\begin{aligned} \mathbb{G}_{\nu,\tau}^z \mathbb{G}_{\nu,\tau}^x \mathbb{J}_{\nu,\tau-1} \mathbb{G}_{\nu,\tau}^x &= \mathbb{G}_{\nu,\tau}^z \mathbb{G}_{\nu,\tau}^x \left[\mathbb{G}_{\nu,\tau-1}^z + \frac{i}{2} [\sigma_{\nu,\tau-1}^z \otimes \sigma_{\nu,\tau}^z - \sigma_{\nu,\tau}^z \otimes \sigma_{\nu,\tau-1}^z] \right] \mathbb{G}_{\nu,t}^x \\ &= \mathbb{G}_{\nu,\tau}^z \mathbb{G}_{\nu,\tau}^x \left[\mathbb{G}_{\nu,\tau}^x \mathbb{G}_{\nu,\tau-1}^z + \frac{i}{4} [\mathbb{1} - \sigma_{\nu,\tau}^x \otimes \sigma_{\nu,\tau}^x] [\sigma_{\nu,\tau-1}^z \otimes \sigma_{\nu,\tau}^z - \sigma_{\nu,\tau}^z \otimes \sigma_{\nu,\tau-1}^z] \right] \\ &= \mathbb{G}_{\nu,\tau}^z \mathbb{G}_{\nu,\tau}^x \mathbb{G}_{\nu,\tau-1}^z. \end{aligned} \quad (\text{F26})$$

We see that (F25) agrees with (F22) for $n = 1$. We then compute

$$\begin{aligned}
\mathbb{A}_{\nu,1}\mathbb{A}_{\nu,2}\mathbb{A}_{\nu,3} &= \mathbb{G}_{\nu,t}^z \mathbb{J}_{\nu,t-1} \mathbb{G}_{\nu,t}^x \mathbb{G}_{\nu,t}^z \mathbb{J}_{\nu,t-1} \mathbb{G}_{\nu,t}^x \mathbb{X}_{\nu,t-1} \mathbb{G}_{\nu,t}^z \mathbb{J}_{\nu,t-1} \mathbb{G}_{\nu,t}^x \mathbb{J}_{\nu,t-2} \tilde{\mathbb{Z}}_{\nu,t-1}^{h_3, \phi_3} \mathbb{X}_{\nu,t-2} \mathbb{X}_{\nu,t-1} \\
&= \mathbb{J}_{\nu,t-1} \mathbb{G}_{\nu,t}^z \mathbb{G}_{\nu,t}^x \mathbb{G}_{\nu,t-1}^z \mathbb{X}_{\nu,t-1} \mathbb{G}_{\nu,t-1}^z \mathbb{J}_{\nu,t-1} \mathbb{G}_{\nu,t}^x \mathbb{J}_{\nu,t-2} \tilde{\mathbb{Z}}_{\nu,t-1}^{h_3, \phi_3} \mathbb{X}_{\nu,t-2} \mathbb{X}_{\nu,t-1} \\
&= \mathbb{J}_{\nu,t-1} \mathbb{G}_{\nu,t}^z \mathbb{G}_{\nu,t}^x \mathbb{G}_{\nu,t-1}^z \mathbb{X}_{\nu,t-1} \mathbb{G}_{\nu,t-1}^z \mathbb{J}_{\nu,t-2} \tilde{\mathbb{Z}}_{\nu,t-1}^{h_3, \phi_3} \mathbb{X}_{\nu,t-2} \mathbb{X}_{\nu,t-1} \\
&= \mathbb{J}_{\nu,t-1} \mathbb{G}_{\nu,t}^z \mathbb{G}_{\nu,t}^x \mathbb{G}_{\nu,t-1}^z \mathbb{G}_{\nu,t-1}^x \mathbb{J}_{\nu,t-2} \tilde{\mathbb{Z}}_{\nu,t-1}^{h_3, \phi_3} \mathbb{X}_{\nu,t-2} \mathbb{X}_{\nu,t-1} \\
&= \mathbb{J}_{\nu,t-1} \mathbb{G}_{\nu,t}^z \mathbb{G}_{\nu,t}^x \mathbb{G}_{\nu,t-1}^z \mathbb{G}_{\nu,t-1}^x \mathbb{J}_{\nu,t-2} \mathbb{X}_{\nu,t-2} \mathbb{X}_{\nu,t-1}.
\end{aligned} \tag{F27}$$

In the last step we used

$$\mathbb{G}_{\nu,\tau}^z \tilde{\mathbb{Z}}_{\nu,\tau}^{h,\phi} = \mathbb{G}_{\nu,\tau}^z. \tag{F28}$$

Since (F27) agrees with (F23) for $n = 1$ we successfully established the basis for the inductive procedure. To conclude we need to prove that

- (i) if (F22) holds for n then (F23) holds for n
- (ii) if (F23) holds for n then (F22) holds for $n + 1$.

Let us prove (i). Assuming (F22) we have

$$\begin{aligned}
\mathbb{A}_{\nu,1} \cdots \mathbb{A}_{\nu,2n} \mathbb{A}_{\nu,2n+1} &= \mathbb{J}_{\nu,t-1} \prod_{j=0}^{n-1} [\mathbb{G}_{\nu,t-j}^z \mathbb{G}_{\nu,t-j}^x] \mathbb{G}_{\nu,t-n}^z \mathbb{X}_{\nu,t-n} \prod_{j=n}^{2n-2} \left[\prod_{\tau=t-1-j}^{t-2n+j} \mathbb{J}_{\nu,\tau} \prod_{\tau=t-j}^{t-2n+j} \tilde{\mathbb{Z}}_{\nu,\tau}^{h_{j+2}, \phi_{j+2}} \prod_{\tau=t-1-j}^{t-2n+j+1} \mathbb{X}_{\nu,\tau} \right], \\
&\quad \times \mathbb{G}_{\nu,t}^z \mathbb{J}_{\nu,t-1} \mathbb{G}_{\nu,t}^x \prod_{\tau=t-2n}^{t-2} \mathbb{J}_{\nu,\tau} \prod_{\tau=t-2n+1}^{t-1} \tilde{\mathbb{Z}}_{\nu,\tau}^{h_{2n+1}, \phi_{2n+1}} \prod_{\tau=t-2n}^{t-1} \mathbb{X}_{\nu,\tau} \\
&= \mathbb{J}_{\nu,t-1} \prod_{j=0}^{n-1} [\mathbb{G}_{\nu,t-j}^z \mathbb{G}_{\nu,t-j}^x] \mathbb{G}_{\nu,t-n}^z \mathbb{X}_{\nu,t-n} \prod_{j=n}^{2n-2} \left[\prod_{\tau=t-1-j}^{t-2n+j} \mathbb{J}_{\nu,\tau} \prod_{\tau=t-j}^{t-2n+j} \tilde{\mathbb{Z}}_{\nu,\tau}^{h_{j+2}, \phi_{j+2}} \prod_{\tau=t-1-j}^{t-2n+j+1} \mathbb{X}_{\nu,\tau} \right], \\
&\quad \times \mathbb{G}_{\nu,t-1}^z \prod_{\tau=t-2n}^{t-2} \mathbb{J}_{\nu,\tau} \prod_{\tau=t-2n+1}^{t-1} \tilde{\mathbb{Z}}_{\nu,\tau}^{h_{2n+1}, \phi_{2n+1}} \prod_{\tau=t-2n}^{t-1} \mathbb{X}_{\nu,\tau}
\end{aligned} \tag{F29}$$

where we used that $\mathbb{G}_{\nu,t}^x$ commutes with all the terms on the first line to bring it close to $\mathbb{J}_{\nu,t-1}$. Then we employed (F26). Moving the projector $\mathbb{G}_{\nu,t-1}^z$ on the second line to the left and using multiple times (F20) and (F26) we have

$$\begin{aligned}
\mathbb{A}_{\nu,1} \cdots \mathbb{A}_{\nu,2n} \mathbb{A}_{\nu,2n+1} &= \mathbb{J}_{\nu,t-1} \prod_{j=0}^{n-1} [\mathbb{G}_{\nu,t-j}^z \mathbb{G}_{\nu,t-j}^x] \mathbb{G}_{\nu,t-n}^z \mathbb{X}_{\nu,t-n} \mathbb{G}_{\nu,t-n}^z \prod_{j=n}^{2n-2} \left[\prod_{\tau=t-1-j}^{t-2n+j-1} \mathbb{J}_{\nu,\tau} \prod_{\tau=t-j}^{t-2n+j-1} \tilde{\mathbb{Z}}_{\nu,\tau}^{h_{j+2}, \phi_{j+2}} \prod_{\tau=t-1-j}^{t-2n+j} \mathbb{X}_{\nu,\tau} \right], \\
&\quad \times \prod_{\tau=t-2n}^{t-2} \mathbb{J}_{\nu,\tau} \prod_{\tau=t-2n+1}^{t-1} \tilde{\mathbb{Z}}_{\nu,\tau}^{h_{2n+1}, \phi_{2n+1}} \prod_{\tau=t-2n}^{t-1} \mathbb{X}_{\nu,\tau} \\
&= \mathbb{J}_{\nu,t-1} \prod_{j=0}^{n-1} [\mathbb{G}_{\nu,t-j}^z \mathbb{G}_{\nu,t-j}^x] \mathbb{G}_{\nu,t-n}^z \mathbb{G}_{\nu,t-n}^x \prod_{j=n}^{2n-2} \left[\prod_{\tau=t-1-j}^{t-2n+j-1} \mathbb{J}_{\nu,\tau} \prod_{\tau=t-j}^{t-2n+j-1} \tilde{\mathbb{Z}}_{\nu,\tau}^{h_{j+2}, \phi_{j+2}} \prod_{\tau=t-1-j}^{t-2n+j} \mathbb{X}_{\nu,\tau} \right], \\
&\quad \times \prod_{\tau=t-2n}^{t-2} \mathbb{J}_{\nu,\tau} \prod_{\tau=t-2n+1}^{t-1} \tilde{\mathbb{Z}}_{\nu,\tau}^{h_{2n+1}, \phi_{2n+1}} \prod_{\tau=t-2n}^{t-1} \mathbb{X}_{\nu,\tau} \\
&= \mathbb{J}_{\nu,t-1} \prod_{j=0}^n [\mathbb{G}_{\nu,t-j}^z \mathbb{G}_{\nu,t-j}^x] \prod_{j=n}^{2n-1} \left[\prod_{\tau=t-1-j}^{t-2n+j-1} \mathbb{J}_{\nu,\tau} \prod_{\tau=t-j}^{t-2n+j-1} \tilde{\mathbb{Z}}_{\nu,\tau}^{h_{j+2}, \phi_{j+2}} \prod_{\tau=t-1-j}^{t-2n+j} \mathbb{X}_{\nu,\tau} \right],
\end{aligned} \tag{F30}$$

which is exactly (F23). Let us now prove (ii). Assuming (F23) we have

$$\begin{aligned}
\mathbb{A}_{\nu,1} \cdots \mathbb{A}_{\nu,2n+1} \mathbb{A}_{\nu,2n+2} &= \mathbb{J}_{\nu,t-1} \prod_{j=0}^n [\mathbb{G}_{\nu,t-j}^z \mathbb{G}_{\nu,t-j}^x] \prod_{j=n}^{2n-1} \left[\prod_{\tau=t-1-j}^{t-2n-1+j} \mathbb{J}_{\nu,\tau} \prod_{\tau=t-j}^{t-2n+j-1} \tilde{\mathbb{Z}}_{\nu,\tau}^{h_{j+2},\phi_{j+2}} \prod_{\tau=t-1-j}^{t-2n+j} \mathbb{X}_{\nu,\tau} \right] \\
&\quad \times \mathbb{G}_{\nu,t}^z \mathbb{J}_{\nu,t-1} \mathbb{G}_{\nu,t}^x \prod_{\tau=t-2n-1}^{t-2} \mathbb{J}_{\nu,\tau} \prod_{\tau=t-2n}^{t-1} \tilde{\mathbb{Z}}_{\nu,\tau}^{h_{2n+2},\phi_{2n+2}} \prod_{\tau=t-2n-1}^{t-1} \mathbb{X}_{\nu,\tau} \\
&= \mathbb{J}_{\nu,t-1} \prod_{j=0}^n [\mathbb{G}_{\nu,t-j}^z \mathbb{G}_{\nu,t-j}^x] \prod_{j=n}^{2n-1} \left[\prod_{\tau=t-1-j}^{t-2n-1+j} \mathbb{J}_{\nu,\tau} \prod_{\tau=t-j}^{t-2n+j-1} \tilde{\mathbb{Z}}_{\nu,\tau}^{h_{j+2},\phi_{j+2}} \prod_{\tau=t-1-j}^{t-2n+j} \mathbb{X}_{\nu,\tau} \right] \\
&\quad \times \mathbb{G}_{\nu,t-1}^z \prod_{\tau=t-2n-1}^{t-2} \mathbb{J}_{\nu,\tau} \prod_{\tau=t-2n}^{t-1} \tilde{\mathbb{Z}}_{\nu,\tau}^{h_{2n+2},\phi_{2n+2}} \prod_{\tau=t-2n-1}^{t-1} \mathbb{X}_{\nu,\tau} \tag{F31}
\end{aligned}$$

where we again used that $\mathbb{G}_{\nu,t}^x$ commutes with all the terms on the first line to bring it close to $\mathbb{J}_{\nu,t-1}$ and employed (F26). Moving now the projector $\mathbb{G}_{\nu,t-1}^z$ on the second line to the left and using (F20) and (F26) we have

$$\begin{aligned}
\mathbb{A}_{\nu,1} \cdots \mathbb{A}_{\nu,2n+2} &= \mathbb{J}_{\nu,t-1} \prod_{j=0}^n [\mathbb{G}_{\nu,t-j}^z \mathbb{G}_{\nu,t-j}^x] \mathbb{G}_{\nu,t-n-1}^z \mathbb{X}_{\nu,t-n-1} \prod_{j=n}^{2n-1} \left[\prod_{\tau=t-1-j}^{t-2n-2+j} \mathbb{J}_{\nu,\tau} \prod_{\tau=t-j}^{t-2n+j-2} \tilde{\mathbb{Z}}_{\nu,\tau}^{h_{j+2},\phi_{j+2}} \prod_{\tau=t-1-j}^{t-2n-1+j} \mathbb{X}_{\nu,\tau} \right] \\
&\quad \times \prod_{\tau=t-2n-1}^{t-2} \mathbb{J}_{\nu,\tau} \prod_{\tau=t-2n}^{t-1} \tilde{\mathbb{Z}}_{\nu,\tau}^{h_{2n+2},\phi_{2n+2}} \prod_{\tau=t-2n-1}^{t-1} \mathbb{X}_{\nu,\tau} \\
&= \mathbb{J}_{\nu,t-1} \prod_{j=0}^n [\mathbb{G}_{\nu,t-j}^z \mathbb{G}_{\nu,t-j}^x] \mathbb{G}_{\nu,t-n-1}^z \mathbb{X}_{\nu,t-n-1} \prod_{j=n}^{2n} \left[\prod_{\tau=t-1-j}^{t-2n-2+j} \mathbb{J}_{\nu,\tau} \prod_{\tau=t-j}^{t-2n+j-2} \tilde{\mathbb{Z}}_{\nu,\tau}^{h_{j+2},\phi_{j+2}} \prod_{\tau=t-1-j}^{t-2n-1+j} \mathbb{X}_{\nu,\tau} \right], \tag{F32}
\end{aligned}$$

which is exactly (F22) for $n+1$. This concludes the proof. \square

-
- | | |
|--|--|
| <p>[1] A. Einstein, B. Podolsky, and N. Rosen, <i>Phys. Rev.</i> 47, 777 (1935).</p> <p>[2] J. S. Bell, <i>Rev. Mod. Phys.</i> 38, 447 (1966).</p> <p>[3] L. Amico, R. Fazio, A. Osterloh, and V. Vedral, <i>Rev. Mod. Phys.</i> 80, 517 (2008).</p> <p>[4] N. Laflorencie, <i>Phys. Rep.</i> 643, 1 (2016).</p> <p>[5] N. Schuch, M. M. Wolf, F. Verstraete, and J. I. Cirac, <i>Phys. Rev. Lett.</i> 100, 030504 (2008).</p> <p>[6] N. Schuch, M. M. Wolf, K. G. H. Vollbrecht, and J. I. Cirac, <i>New J. Phys.</i> 10, 033032 (2008).</p> <p>[7] A. Perales and G. Vidal, <i>Phys. Rev. A</i> 78, 042337 (2008).</p> <p>[8] P. Hauke, F. M. Cucchietti, L. Tagliacozzo, I. Deutsch, and M. Lewenstein, <i>Prog. Phys.</i> 75 082401 (2012).</p> <p>[9] J. Dubail, <i>J. Phys. A</i> 50, 234001 (2017).</p> <p>[10] P. Calabrese, <i>Physica A</i> 504, 31-44 (2018).</p> <p>[11] J. M. Deutsch, H. Li, and A. Sharma, <i>Phys. Rev. E</i> 87, 042135 (2013).</p> <p>[12] W. Beugeling, A. Andreanov, and M. Haque, <i>J. Stat. Mech.</i> (2015) P02002.</p> <p>[13] V. Gurarie, <i>J. Stat. Mech.</i> (2013) P02014.</p> <p>[14] L. F. Santos, A. Polkovnikov, and M. Rigol, <i>Phys. Rev. Lett.</i> 107, 040601 (2011).</p> <p>[15] P. Calabrese and J. Cardy, <i>J. Stat. Mech.</i> (2005) P04010.</p> | <p>[16] G. De Chiara, S. Montangero, P. Calabrese and R. Fazio, <i>J. Stat. Mech.</i> (2006) P03001.</p> <p>[17] M. Fagotti and P. Calabrese, <i>Phys. Rev. A</i> 78, 010306(R).</p> <p>[18] V. Eisler and I. Peschel, <i>Ann. Phys. (Berlin)</i> 17, 410 (2008).</p> <p>[19] M. G. Nezhadhighi and M. A. Rajabpour, <i>Phys. Rev. B</i> 90, 205438 (2014).</p> <p>[20] L. Bucciantini, M. Kormos, and P. Calabrese, <i>J. Phys. A</i> 47, 175002 (2014).</p> <p>[21] E. Bianchi, L. Hackl, and N. Yokomizo, <i>N. J. High Energy Phys.</i> (2018) 2018: 25.</p> <p>[22] L. Hackl, E. Bianchi, R. Modak, and M. Rigol, <i>Phys. Rev. A</i> 97, 032321 (2018).</p> <p>[23] M. Fagotti and M. Collura, arXiv:1507.02678.</p> <p>[24] A. S. Buyskikh, M. Fagotti, J. Schachenmayer, F. Essler, and A. J. Daley, <i>Phys. Rev. A</i> 93, 053620 (2016).</p> <p>[25] J. S. Cotler, M. P. Hertzberg, M. Mezei, and M. T. Mueller, <i>JHEP</i> 11, 166 (2016).</p> <p>[26] V. Alba and P. Calabrese, <i>PNAS</i> 114, 7947-7951 (2017); V. Alba and P. Calabrese, <i>SciPost Phys.</i> 4, 017 (2018).</p> <p>[27] M. Mestyan, B. Bertini, L. Piroli, and P. Calabrese, <i>J. Stat. Mech.</i> (2017) 083103.</p> |
|--|--|

- [28] C. Pascu Moca, M. Kormos, and G. Zarand, *Phys. Rev. Lett.* **119**, 100603 (2017).
- [29] I. Frerot, P. Naldesi, and T. Roscilde, *Phys. Rev. Lett.* **120**, 050401 (2018).
- [30] M. Collura, M. Kormos, and G. Takacs, *Phys. Rev. A* **98**, 053610 (2018).
- [31] B. Bertini, E. Tartaglia, and P. Calabrese, *J. Stat. Mech.* (2018) 063104.
- [32] A. Bastianello, P. Calabrese, *SciPost Phys.* **5**, 033 (2018).
- [33] H. Liu and S. J. Suh, *Phys. Rev. Lett.* **112**, 011601 (2014).
- [34] H. Casini, H. Liu, and M. Mezei, *J. High Energy Phys.* **07** (2016) 077.
- [35] C.T. Asplund, A. Bernamonti, F. Galli, T. Hartman, *J. High Energy Phys.* **09** (2015) 110.
- [36] S. Leichenauer and M. Moosa, *Phys. Rev. D* **92**, 126004 (2015).
- [37] V. Alba, *Phys. Rev. B* **97**, 245135 (2018).
- [38] B. Bertini, M. Fagotti, L. Piroli, and P. Calabrese, *J. Phys. A: Math. Theor.* **51**, 39LT01 (2018).
- [39] A. J. Daley, H. Pichler, J. Schachenmayer, and P. Zoller, *Phys. Rev. Lett.* **109**, 020505 (2012).
- [40] A. Elben, B. Vermersch, M. Dalmonte, J. I. Cirac, and P. Zoller, *Phys. Rev. Lett.* **120**, 050406 (2018).
- [41] A. Laeuchli and C. Kollath, *J. Stat. Mech.* P05018 (2008).
- [42] H. Kim and D. A. Huse, *Phys. Rev. Lett.* **111**, 127205 (2013).
- [43] R. Pal and A. Lakshminarayan, [arXiv:1805.11632](https://arxiv.org/abs/1805.11632) (2018).
- [44] A. M. Kaufman, M. E. Tai, A. Lukin, M. Rispoli, R. Schittko, P. M. Preiss, and M. Greiner, *Science* **353**, 794 (2016).
- [45] M. Žnidarič, T. Prosen and P. Prelovšek, *Phys. Rev. B* **77**, 064426 (2008).
- [46] M. Kormos, M. Collura, G. Takács, and P. Calabrese, *Nature Physics* **13**, 246 (2017).
- [47] A. Nahum, J. Ruhman, and D. A. Huse, *Phys. Rev. B* **98**, 035118 (2018).
- [48] R. Nandkishore and D. A. Huse, *Annu. Rev. Condens. Matter Phys.* **6**, 15 (2015).
- [49] A. Nahum, J. Ruhman, S. Vijay, and J. Haah, *Phys. Rev. X* **7**, 031016 (2017).
- [50] C. von Keyserlingk, T. Rakovszky, F. Pollmann, and S. Sondhi, *Phys. Rev. X* **8**, 021013 (2018).
- [51] A. Nahum, S. Vijay, and J. Haah, *Phys. Rev. X* **8**, 021014 (2018).
- [52] C. Jonay, D. A. Huse, and A. Nahum, [1803.00089](https://arxiv.org/abs/1803.00089).
- [53] T. Zhou and A. Nahum, [1804.09737](https://arxiv.org/abs/1804.09737).
- [54] A. Chan, A. De Luca, J. T. Chalker, *Phys. Rev. X* **8**, 041019 (2018).
- [55] B. Bertini, P. Kos, and T. Prosen, *Phys. Rev. Lett.* *in press*, [arXiv:1805.00931](https://arxiv.org/abs/1805.00931) (2018).
- [56] Note that the notions “quantum chaotic” and “ergodic” are equivalent for a quantum many-body system and are used interchangeably in the paper.
- [57] T. Prosen, *Phys. Rev. E*, **65**, 036208 (2002).
- [58] T. Prosen, *J. Phys. A* **35**, L737 (2002).
- [59] T. Prosen, *J. Phys. A* **40**, 7881 (2007).
- [60] C. Pineda and T. Prosen, *Phys. Rev. E* **76**, 061127 (2007).
- [61] I. Bloch, J. Dalibard, and W. Zwerger, *Rev. Mod. Phys.* **80**, 885 (2008).
- [62] P. Bordia, H. Lüschen, U. Schneider, M. Knap, and I. Bloch, *Nature Physics* **13**, 460-464 (2017)
- [63] J. Zhang, P. W. Hess, A. Kyprianidis, P. Becker, A. Lee, J. Smith, G. Pagano, I.-D. Potirniche, A. C. Potter, A. Vishwanath, N. Y. Yao, and C. Monroe, *Nature* **543**, 217-220 (2017).
- [64] M. Akila, D. Waltner, B. Gutkin, and T. Guhr, *J. Phys. A* **49**, 375101 (2016).
- [65] Note that for $\theta_j \in \{0, \pi\}$ the states (11) are independent of ϕ . This means that we do not need to specify the value of ϕ in (16).
- [66] Note that a similar “dual route” has also been proposed in the context of tensor networks techniques in: M. C. Bañuls, M. B. Hastings, F. Verstraete, and J. I. Cirac, *Phys. Rev. Lett.* **102**, 240603 (2009).
- [67] D. N. Page, *Phys. Rev. Lett.* **71**, 1291 (1993).
- [68] L. Vidmar and M. Rigol, *Phys. Rev. Lett.* **119**, 220603 (2017).
- [69] S. Sotiriadis, *Phys. Rev. A* **94**, 031605 (2016).
- [70] M. Gluza, C. Krumnow, M. Friesdorf, C. Gogolin, and J. Eisert, *Phys. Rev. Lett.* **117**, 190602 (2016).